AD NUMBER

AD822785

NEW LIMITATION CHANGE

TO

Approved for public release, distribution unlimited

FROM

Distribution authorized to U.S. Gov't. agencies only; Test and Evaluation; DEC 1971. Other requests shall be referred to Air Force Flight Dynamics Lab., Attn: FY, Wright-Patterson AFB, OH 45433.

AUTHORITY

AFFDL ltr dtd 13 Oct 1975

AFFDL-TR-67-37

PROPAGATION OF HIGH INTENSITY SOUND WAVES

HENRY B. KARPLUS
VERNER J. RAELSON
GALE R. HRUSKA

IIT RESEARCH INSTITUTE

TECHNICAL REPORT AFFDL-TR-67-37

SEPTEMBER 1967

AIR FORCE FLIGHT DYNAMICS LABORATORY
RESEARCH AND TECHNOLOGY DIVISION
AIR FORCE SYSTEMS COMMAND
WRIGHT-PATTERSON AIR FORCE BASE, OHIO

NOTICE

When Government drawings, specifications, or other data are used for any purpose other than in connection with a definitely related Government procurement operation, the United States Government thereby incurs no responsibility nor any obligation whatsoever; and the fact that the Government may have formulated, furnished, or in any way supplied the said drawings, specifications, or other data, is not to be regarded by implication or otherwise as in any manner licensing the holder or any other person or corporation, or conveying any rights or permission to manufacture, use, or sell any patented invention that may in any way be related thereto.

Copies of this report should not be returned unless return is required by security considerations, contractual obligations, or notice on a specific document.

200 - November 1967 - CO455 - 13-267

PROPAGATION OF HIGH INTENSITY SOUND WAVES

HENRY B. KARPLUS
VERNER J. RAELSON
GALE R. HRUSKA

IIT RESEARCH INSTITUTE

FOREWORD

This report was prepared by IIT Research Institute for the Aero-Acoustics Branch, Vehicle Dynamics Division, AF Flight Dynamics Laboratory, Wright-Patterson Air Force Base, Ohio under Contract AF33(615)-3436. This effort is part of the Air Force Systems Command's exploratory development program. This contract was initiated under Project 4437 "High Intensity Sound Environment Simulation", Task 443701 "Sonic Facility Development". Messrs. B. Frock and C. L. Rupert of the Aero-Acoustics Branch were task engineers.

The period covered in this contract is from January 1966 to February 1967.

The project was under the direction of V. J. Raelson who left the IIT Research Institute in October 1966. Mr. Raelson continued as a consultant and wrote Sections 4 and 9. Sections 5, 6, 7, and 8 were written by G. Hruska and edited by V. J. Raelson. Sections 1, 2, 3, 10, 11, and 12 were written and integrated into the report by H. B. Karplus. IITRI Project No. is M-6141.

Manuscript was released by authors, May 1, 1967, for publication as an AFFDL Technical Report

This technical report has been reviewed and is approved.

Howard A. Magrath

HOWARD A. MAGRATH
Chief, Vehicle Dynamics Division
AF Flight Dynamics Laboratory

ABSTRACT

Sound field characteristics were studied as a function of increasing intensity. It was determined that one effect outweighs others. This is the distortion generated within the siren which makes it impossible to generate pure tones above a certain intensity. At high intensity the waveform of the sound assumes a sawtooth shape producing periodic shock waves. Conversely, it is concluded that if the distortion is small at the mouth of the siren, additional distortion in the subsequent propagation will not be significant. Waveforms observed in the AFFDL facility are included in an appendix.

Interaction of sound waves from different sirens will, in addition, give rise to intermodulation effects producing sum and difference frequencies. In general, the intensity in the region in which the radiation from different sirens can interact will be so much lower than the intensity in the throat of the siren horn that these effects will also be small compared with harmonic distortion generated in the sirens.

TABLE OF CONTENTS

TABLE OF CONTENTS (Cont'd)

LIST OF ILLUSTRATIONS

LIST OF ILLUSTRATIONS (Cont'd)

LIST OF TABLES

SUMMARY OF MOST FREQUENTLY USED SYMBOLS

A $= \beta/c_o^2$

$\underline{A}$ $= v_1 w_o^2 \, (w_o^2 + 1)^{-1/2}$

b effective viscosity $= \nu'_n \rho$

$\overline{B}$ $= \exp \, (U_1/2C\omega_1 A + U_2 \cos \delta/2C\omega_2 A)$

C $= \nu' c_o/2\beta^2$

C_p specific heat at constant pressure

C_v specific heat at constant volume

c velocity of sound

c_o velocity of sound for small amplitudes $= (\gamma p_o/\rho_o)^{1/2}$

$\text{erf}( )$ error function

f frequency

f_c cut off frequency of exponential horn

$I_\nu( )$ modified Bessel function

$J_n( )$ Bessel function of the first kind

k heat conductivity

L sound pressure level $= 20 \log_{10} p_{rms} + 74$

m flare constant of exponential horn

p pressure

p_o atmospheric pressure

p_m peak acoustic pressure

p_{rms} root mean square acoustic pressure measured in dynes cm^{-2}

P_r Prandtl number $= \eta C_p/k = 0.71$ for air

$R( )$ autocorrelation function

$\underline{S}( )$ power spectral density

SUMMARY OF MOST FREQUENTLY USED SYMBOLS (Cont'd)

S_t cross section at area of throat of horn

S_m cross section at area of mouth of horn

r distance in spherical coordinates

t time

t' retarded time = $t - x/c_o$

U particle velocity

U_m maximum particle velocity

v = U/c_o

x distance

x_c shock formation distance of lossless plane waves
= $\gamma p_o c_o/\beta\omega p_m$

w = $2\pi r/\lambda$ = normalized distance

y = xC

α classical attenuation = $\nu'\omega^2/c_o^3$

β nonlinearity coefficient = $(\gamma+1)/2$ = 1.2 (for air)

γ = C_p/C_v

δ phase between waves

η shear viscosity

η' dilatational viscosity ($\simeq 0.8\eta$ for nitrogen)

ν kinematic shear viscosity = η/ρ = 0.15 for air

ν' modified effective kinematic viscosity
= $\nu[1 + \eta/2\eta' + (\gamma-1)/2P_r] \simeq 0.23$ cm^2/sec for air

ν'_n = $\nu[4/3 + \eta/2\eta' + (\gamma-1)/2P_r]$

ρ density

σ = x/x_c

λ wavelength

PROPAGATION OF HIGH INTENSITY SOUND WAVES

1. INTRODUCTION

The Air Force Flight Dynamics Laboratory operates a large facility for testing airplane structures in intense sound fields. Very high intensity sound fields are produced by banks of sirens, the level reaching up to about 170 db in the vicinity of the mouth of the siren. The question arose whether this high intensity modifies the low amplitude assumptions normally made when computing sound pressure levels and whether the nonlinear effects of the medium, that is, the air in the facility will introduce effects not accounted for by the normal small amplitude theory. A project was set up with IIT Research Institute under Contract No. AF 33(615)-3436 to study possible effects due to nonlinearities of the air in the facility as normally operated. Effort was predominantly directed toward computation of the magnitude of nonlinear effects from equations obtained from the literature. In addition, where necessary, derivations were directed toward establishment of possible effects not found in the open literature. A small program was also run on determining experimentally the effects of high intensity broadband noise as measured in an acoustic tube. These measurements were further augmented by a few measurements made by the Air Force Flight Dynamics Laboratory in their own facility with two of the sirens running. Waveforms observed in the AFFDL facility are shown in Appendix A.

2. PHYSICAL DESCRIPTION OF THE HIGH INTENSITY EFFECTS

For the small amplitude acoustic approximation of the propagation of pressure disturbances through a fluid it is assumed that the pressure fluctuation is small compared to the ambient pressure and that the instantaneous particle velocity is small compared with the propagation velocity of the disturbance. These assumptions relate to the equation of propagation:

$$c^2 p'' = \ddot{p} \tag{2.1}$$

The second derivative of the pressure with respect to distance, p'', is related to the second derivative with respect to time, $\ddot{p}$, by the propagation velocity squared. The most predominant effect for moderate finite amplitudes is the influence of the instantaneous particle velocity on the sound velocity. The sound velocity is no longer a constant but is the sum of the instantaneous particle velocity and the local sound velocity. In addition, the local sound velocity increases in the regions of high pressure due to the adiabatic heating of the medium and decreases due to the adiabatic cooling in the low pressure region. In this manner the sound velocity, c, is no longer a constant, c_o, but is related to instantaneous particle velocity, U, by Eq.(2.2).

$$c = c_o + \beta U \tag{2.2}$$

where $\beta = (\gamma + 1)/2$ and γ is the ratio of specific heat at constant pressure to the specific heat at constant volume.

2.1 DISTORTION

The higher propagation velocity in regions of positive pressures causes these regions to overtake the regions of low pressures causing a distortion or change of waveform as the pressure disturbances are propagated through the medium. If we start with a pure sinusoidal pressure fluctuation, as shown in

Fig. 2.1(a), the overtaking of the high pressure regions will cause a change in the waveform, as shown in Fig. 2.1(b). Solution of the simple plane wave propagation equation, Eq. (2.1), with c not a constant leads to a rather physically impossible situation, shown by the dotted line in Fig. 2.1(c), where mathematically a double valued pressure exists when the positive pressure displacement has overtaken the negative pressure displacement. This difficulty arises only when no loss mechanism exists in the medium. However, in spherical spreading or in the tapered section of the horn, this difficulty is not important because the drop of intensity with propagation eliminates this difficulty. However, in plane wave propagation if there is no loss mechanism as postulated, the mathematical solution is a physical impossibility and a loss mechanism must be introduced to the equations. Ultimately the waveform assumes the shape shown by the solid line in Fig. 2.1(c), in which a shock wave forms, indicated by the vertical lines in a pressure-space or pressure-time diagram. In summary then, the sinusoidal disturbance of pressure propagating with large amplitude eventually changes its shape to a sawtooth form as shown by the solid line in Fig. 2.1(c) and remains fairly stable in this form, decaying due to the essential loss mechanisms in the medium.

2.2 INTERMODULATION

There is an additional effect on propagation when sound waves of two different frequencies (f_1 and f_2) interact in a region where the medium is not linear and where amplitudes are sufficiently large that nonlinear effects must be taken into account. The high frequencies, f_1, move at a higher velocity when superimposed with a pressure peak of the low frequency, f_2, than when superimposed on a pressure trough of the low frequency. This causes a frequency modulation of the high frequency sound wave as shown in Fig. 2.2. Frequency modulation, of course,

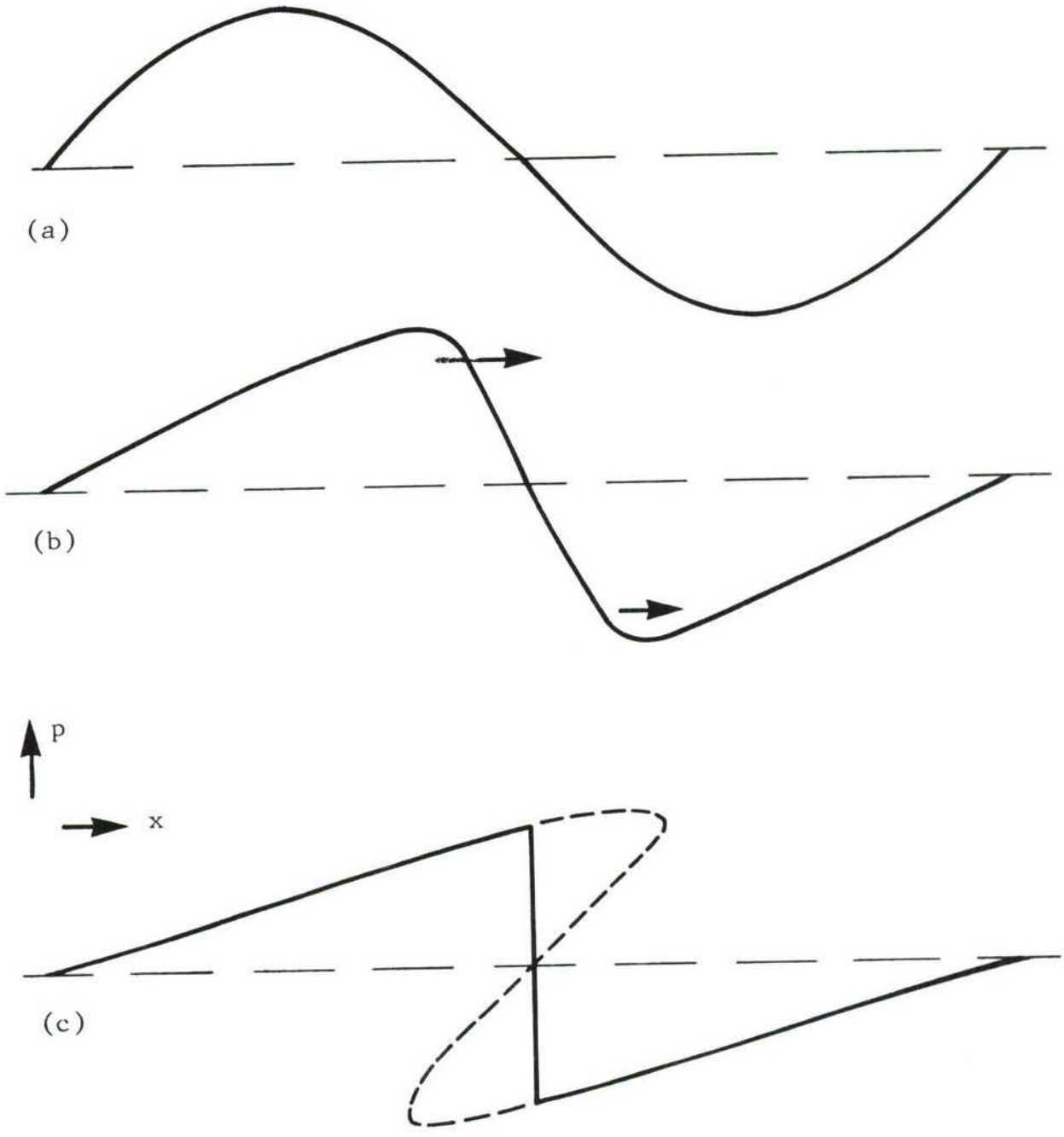

Fig. 2.1. Distortion Generated at Large Amplitudes.

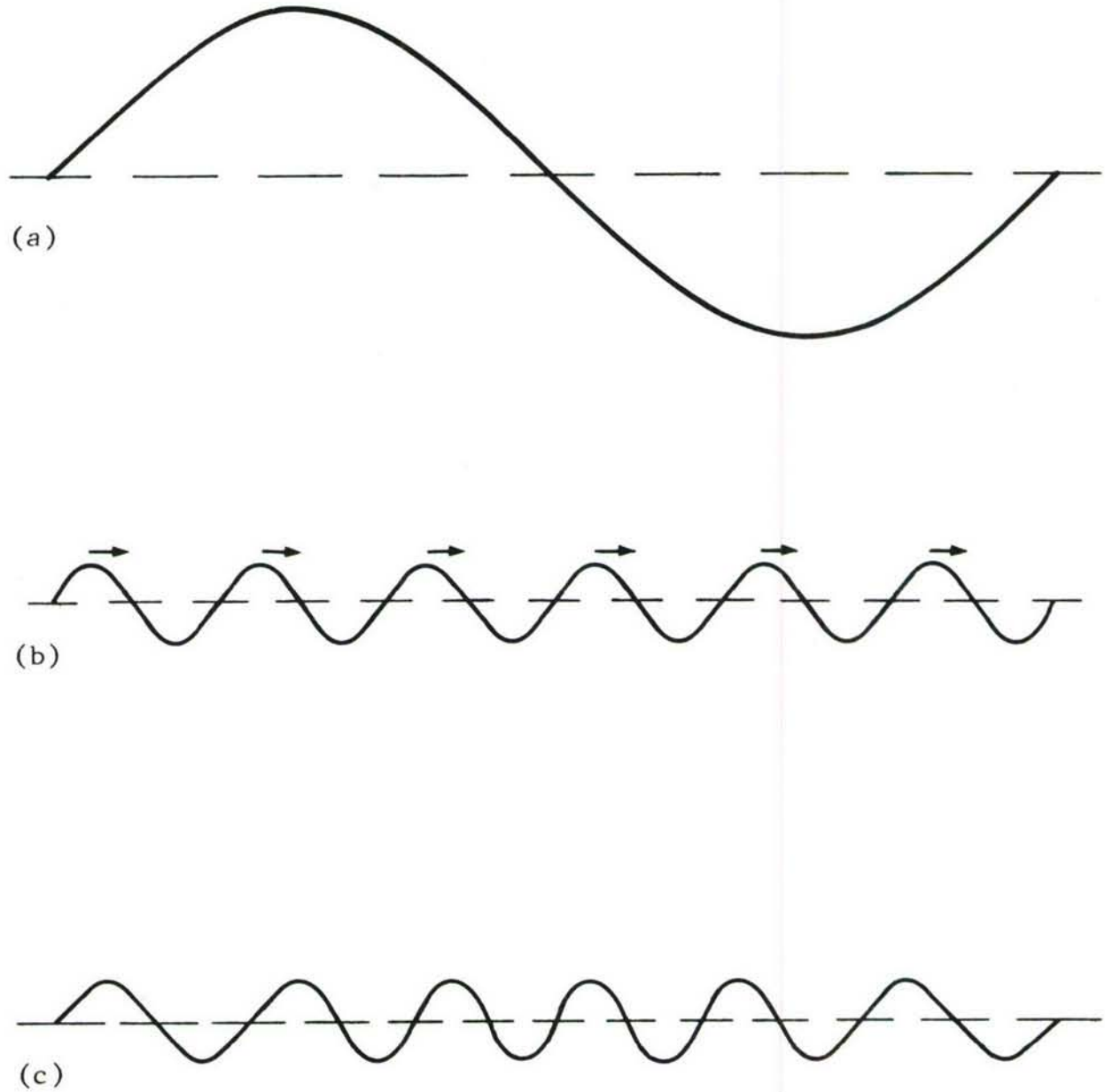

Fig. 2.2. The High Frequency Wave (b) Superimposed on the Large Amplitude Low Frequency Wave Travels with Periodically Varying Velocity Resulting in a Frequency Modulation as at (c).

can be written in terms of mean frequency, f_1, with side bands spaced around this mean frequency at intervals of the modulating low frequency $f_1 \pm nf_2$. This effect occurs only at points outside the siren in the room itself. The most significant region will be the region of spherical spreading. However, for simplicity a plane wave interaction series has been developed. This interaction occurs at considerably lower intensity than the distortion producing intensity in the throat of the horn. For this reason this effect is considerably less than the distortion effect described above.

2.3 BASIS FOR THE MATHEMATICAL FORMULATION

Sound propagation is, for convenience, subdivided into three distinct regions:

1. Exponential spreading inside the horn. This region of propagation is treated in Section 3.
2. Spherical spreading at considerable distances from the sources. The wave front will be a reasonably good approximation to a sphere at distances greater than about a^2/λ, where a^2 is the area of the horn mouth and λ is the wavelength. This region is discussed in more detail in Section 4.
3. There is a short intermediate region immediately outside the sirens where the wave propagates essentially as a plane wave. This region is discussed in Section 5.

Interactions of waves of different frequencies are discussed in Section 6 and effects of reflection in Section 7. The effects of finite bandwidth are discussed in Section 8 and some experimental results on these are given in Section 9. This is followed by a brief discussion of the effects of the wall treatment in the room in Section 10. Recommendations and conclusions are given in Sections 11 and 12.

To compute the local sound velocity c in terms of the small amplitude sound velocity c_o and the particle velocity U or instantaneous acoustic pressure p, and ambient pressure p_o:

$$c_o^2 = \gamma p_o/\rho_o \quad , \tag{2.3}$$

$$c_1 = (\gamma p_1/\rho_1)^{1/2} + U \quad .$$

Hence

$$\frac{c_1}{c_o} = \left[\frac{p_1}{\rho_1}\,\frac{\rho_o}{p_o}\right]^{1/2} + \frac{U_1}{c_o} \quad .$$

Substituting the adiabatic relation

$$p_1\rho_1^{-\gamma} = p_o\rho_o^{-\gamma} \quad ,$$

$$\frac{c_1}{c_o} = \frac{p_1}{p_o}^{(\gamma-1)/2\gamma} + \frac{U_1}{c_o} \quad . \tag{2.4}$$

If the pressure amplitude is still sufficiently small that the binomial expansion may be limited to the first term

$$\frac{p_1}{p_o}^{(\gamma-1)/2\gamma} = \left[\frac{p_1 - p_o}{p_o} + 1\right]^{(\gamma-1)/2\gamma}$$

$$\simeq 1 + \frac{\gamma - 1}{2\gamma}\,\frac{p_1 - p_o}{p_o} \quad . \tag{2.5}$$

Now the excess pressure, $p = p_1 - p_o$, is related to the particle velocity U_1 by the medium impedance ρc_o.

$$U_1\rho c_o = p \quad , \tag{2.6}$$

or

$$\frac{p}{p_o} \simeq U_1\rho_o c_o/p_o = \frac{\gamma U_1 c_o}{c_o^2} = \frac{\gamma U_1}{c_o} \quad . \tag{2.7}$$

Substituting Eq. (2.7) in Eq. (2.5) and this in Eq. (2.4) gives

$$c_1 = c_o + \beta U \qquad (2.8)$$

where $\beta = (\gamma + 1)/2$.

This is the nonlinear effect valid for moderate sound pressures ($p_1 - p_o \ll p_o$) with which all treatments of nonlinear acoustics start.

We further compute the conditions necessary for the formation of shock waves, Fig. 2.1(c). To treat three separate regions (plane waves, spherical waves, and the exponential expansion within the horn), we start off with a general change of sound pressure with distance.

$$p = R(x)\, p_m \sin \omega(t - x/c) \quad .$$

It is possible to substitute various specific functions for the different propagation regions. For plane waves, neglecting absorption:

$$R(x) = 1 \quad . \qquad (2.9)$$

If absorption is taken into account:

$$R(x) = e^{-\alpha x} \quad ; \qquad (2.10)$$

in general, the absorption coefficient α is a function of frequency. In the development in Section 5, the absorption computed on the bases of heat conduction and viscosity is used. The results there presented are valid for dry air. The presence of water vapor introduces an additional variable leading to higher absorption especially in the upper frequency region under consideration.

In the region within an exponential horn having a flare constant m: $S_x = S_t e^{mx}$ the sound pressure function becomes:

$$R(x) = e^{-mx/2} \quad . \qquad (2.11)$$

In the region of spherical spreading the intensity decreases as the inverse square of the distance and the sound pressure decreases as the inverse first power:

$$R(x) = r_o/x \quad . \tag{2.12}$$

Both within the horn and where sound radiation diverges spherically, the intensity reduction due to the increasing area of the wave front greatly exceeds the internal losses. The latter are, therefore, of paramount importance only for plane waves.

The condition for the formation of shock waves is then expressed mathematically as the rate of change of the pressure with distance becoming very large

$$dp/dx \rightarrow \infty \quad . \tag{2.13}$$

We utilize the relations between particle velocity, sound velocity, and pressure:

$$c = c_o + \beta U \quad , \tag{2.8}$$

$$p = U\rho c_o \quad , \tag{2.6}$$

$$dp = \rho c_o dU = (\rho c_o/\beta)\, dc \quad . \tag{2.14}$$

Furthermore, the propagation of an initially simple harmonic wave of pressure amplitude p_m is

$$p = p_m R(x) \sin \omega (t-x/c) \quad . \tag{2.15}$$

$$\begin{aligned} dp &= \left(\frac{\partial p}{\partial x}\right)_c dx + \left(\frac{\partial p}{\partial c}\right)_x dc \\ &= \left(\frac{\partial p}{\partial x}\right)_c dx + \left(\frac{\partial p}{\partial c}\right)_x \frac{\beta}{\rho c_o} dp \quad , \end{aligned} \tag{2.16}$$

$$\therefore \quad \frac{dp}{dx}\left[1 - \frac{\beta}{\rho c_o}\left(\frac{\partial p}{\partial c}\right)_x\right] = \left(\frac{\partial p}{\partial x}\right)_c . \tag{2.17}$$

When

$$\left(\frac{\partial p}{\partial c}\right)_x \frac{\beta}{\rho c_o} = 1 , \tag{2.18}$$

$$dp/dx \rightarrow \infty$$

and shock waves form.

Now differentiate Eq. (2.15):

$$\left(\frac{\partial p}{\partial c}\right)_x = p_m R(x) \cos[\omega (t-x/c)](x\omega/c^2) . \tag{2.19}$$

The largest possible value of a cosine function is unity, so that by substituting Eqs. (2.18) in (2.19) we conclude that shock conditions begin to appear when

$$p_m R(x) \frac{x\omega}{c^2} \frac{\beta}{\rho c_o} \geq 1 . \tag{2.20}$$

The sound velocity is assigned the mean value:

$$c \simeq c_o . \tag{2.21}$$

For the plane wave condition without attenuation by Eq. (2.9): $R(x) = 1$, so that substituting Eq. (2.9) and (2.21) in Eq. (2.20):

$$x_c \geq \frac{\rho c_o^3}{p_m \beta\omega} = \frac{\gamma p_o c_o}{p_m 2\pi f\beta} = 6.3 \times 10^3 \frac{p_o}{p_m} \frac{1}{f} \text{ [cm]} \tag{2.22}$$

This is the shock formation distance.

Table 2.1 gives the shock formation distance for plane wave propagation in terms of frequency in kHz and sound pressure level $20 \log \sqrt{1/2}\ p_m/0.0002$. The plane wave region a^2/λ is given for comparison, for the particular sirens a = 1 ft.

TABLE 2.1

SHOCK FORMATION DISTANCE IN FEET

Sound Pressure Level, db	p_m dynes/cm^2	Frequency, kHz 0.1	0.3	1	3	10
171	10^5	21	7	2.1	0.7	0.21
165	5×10^4	42	14	4.2	1.4	0.42
157	2×10^4	105	35	10.5	3.5	1.05
151	10^4	210	70	21	7	2.1
(a = 1 ft) a^2/λ		0.1	0.3	1	3.3	10

From this table it appears that below 1 kHz the plane wave generated at the mouth of a 1 ft square source would start to spread and become a spherical wave before shock waves form. On the other hand, if horns are redesigned so that they can produce reasonable pure wave forms at over 3 kHz, shocks may form in front of the siren.

For the condition of propagation in a horn, Eqs. (2.11) and (2.18) give:

$$p_m \omega x e^{-mx/2} \beta/\rho c_o^3 \geq 1 \quad .$$

Now the quantity $xe^{-mx/2}$ has a maximum value $2/me$ when $x = 2/m$. This means either shocks form for $x < 2/m$ or they will never form. (Note: at the point $x = 2/m$ the cross-sectional area of the horn is $\overline{e}^2 (= 7.36)$ times the area of the throat.) The maximum peak pressure in the throat must be

$$p_m \geq \frac{\rho c_o^3}{\beta \omega} \frac{me}{2} \quad . \tag{2.23}$$

Using the concept of the cut off frequency, f_c, below which the horn is a very ineffective radiator

$$f_c = mc_o/4\pi \tag{2.24}$$

gives

$$p_m \geq \frac{\rho c_o^2}{\beta} \frac{f_c}{f} e = \frac{\gamma p_o e}{\beta} \frac{f_c}{f} = \frac{f_c}{f} \times 3.16 \times 10^6 \text{ dynes cm}^{-2} \tag{2.25}$$

Table 2.2 gives the sound pressure level at the throat of the horn for shock wave production as a function of the ratio of frequency, f, to the horn cut off frequency, f_c.

TABLE 2.2

SOUND PRESSURE LEVEL AT THE THROAT OF THE HORN

f/f_c	1	2	5	10	20	50	
$20 \log[\sqrt{0.5}\, p_m/0.0002]$	201	198	194	191	188	184	db

For spherical radiation, Eq. (2.12): $R(x) = r_o/x$ and Eq. (2.20) yield for the condition for shock formation:

$$p_m \geq \frac{\rho c_o^3}{\beta\omega r_o} = \frac{\gamma p_o c_o}{\beta\omega r_o} \tag{2.26}$$

$$= \frac{6.2}{Fr_o} \times 10^5 \text{ dynes cm}^{-2} \tag{2.27}$$

where F is the frequency in kHz and r_o the radius of the wave front where the sound pressure is p_m.

It is now necessary to relate the sound pressure level at some distance r_o where propagation has developed to a spherical form to the sound pressure, p_g, at the mouth of the horn.

If losses are neglected, then the total sound power through a hemisphere of radius r_o is equal to the sound power from the mouth of the horn.

$$\frac{p_g^2 S_m}{2\pi r_o^2 p_m^2} = 1 \qquad (2.28)$$

$$\therefore\ p_g = p_m r_o \sqrt{2\pi/S_m} \ .$$

So that conditions for shock waves forming in the region of spherical spreading becomes

$$p_g = \frac{\gamma P_o c_o}{\beta\omega} \frac{\sqrt{2\pi}}{\sqrt{S_m}} \ . \qquad (2.29)$$

Substituting for the area of the mouth (1 ft^2):

$$S_m = (30.4)^2 \text{ cm}^2 \qquad (2.30)$$

$$p_g \geq 5.45 \times 10^5/F \text{ dynes cm}^{-2}$$

Table 2.3 gives the sound pressure level L_g in db re 0.0002 dynes cm^{-2} at the mouth of a horn as a function of frequency in kHz below which no shock formation in the region of spherical spreading is expected.

TABLE 2.3

SOUND PRESSURE LEVELS AT THE MOUTH OF THE HORN ABOVE WHICH SHOCK WAVES WILL FORM IN THE REGION OF SPHERICAL SPREADING

F, kHz	0.1	0.2	0.5	1	2	5	10
L_g, db	196	193	189	186	183	179	176

Comparison of this table with Table 2.2 shows that shock formation in the region of spherical spreading will not occur with sirens of presently available power. Thus, if sirens are modified to have a higher cut off frequency so that the formation of shock waves in the horns is avoided, then shock formation in the short plane wave region immediately in front of the sirens is the most important consideration. Table 2.3 indicates that shock formation in the region of spherical spreading need not be considered. A more precise treatment of shock formation under conditions of spherical spreading is considered in Section 4. The assumption that radiation immediately in front of the horn approaches plane waves is a reasonably good assumption for the horns of current design, having a large center core. If horns with higher cut off frequencies are designed, this assumption should be reviewed.

2.4 GROWTH OF DISTORTION IN PLANE WAVE PROPAGATION OF INITIALLY SIMPLE HARMONIC WAVES

The growth of harmonics in plane waves has been computed taking full account of absorption by Blackstock[1] and by Cook.[2] The method of computation was different and Blackstock states that his results were sufficiently close to those of Cook that he found it not worth while reporting the results. In both cases digital computer techniques were used. In both cases the rate of growth of harmonics was computed as a function of the product of absorption coefficient of the fundamental (Blackstock: α; Cook: α_o) and the shock formation distance (Cook: $L = x_c$ in Section 2.4, Eq. 2.22 of this report). Blackstock calls the function $\alpha_o L = \Gamma^{-1}$. Blackstock extended computation over the range $0.2 < \Gamma < 100$. Cook showed that, prior to the formation of a shock the growth of harmonics for $\alpha_o L < 0.01$, ($\Gamma > 100$), (Ref. 2, Fig. 9.11), the function of the rate of growth of harmonics is substantially the same as that computed much more simply independently by Fubini-Ghiron[3], by Keck and Beyer[4], and by Hargrove[5] for the condition $\alpha_o = 0$.

Inserting into the expression for αx_c values to be expected in the operating range of the facility under consideration

$$\alpha = \nu' \omega^2 / c_o^3 \tag{2.31}$$

where $\nu' = \nu \left[1 + \eta'/2\eta + (\gamma-1)/2P_r\right]$

ν = kinematic viscosity $\simeq$ 0.15 for air at 70°F

η'/η = ratio of dilations to shear viscosity

= 0.8 for air

P_r = Prandtl number = 0.71

Hence, using Eq. (2.22)

$$\alpha x_c = \nu' \frac{\gamma p_o 2\pi f}{p_m \beta c_o^2} \tag{2.32}$$

$$= \frac{0.251 \times 1.4 \times 1.01 \times 10^6 \times 6.28}{1.2 \times (3.44)^2 \times 10^8} \frac{f}{p_m}$$

$$= 1.58 \times 10^{-3} \, f/p_m \tag{2.33}$$

Now in the problem under consideration $f < 10^4$ and $p_m > 10^4$ (151 db) (for lower sound pressures the nonlinear effects are small); so that in the range of interest for the facility $\alpha x_c < 0.01 << 1$. Therefore, in the region prior to the formation of a shock the attenuation is negligible and the simple expression for the intensity of harmonics of Fubini-Ghiron[3], Keck and Beyer[4], or Hargrove[5] is accurate to better than about 1 db.

$$p = p_m \sum_{n=1}^{\infty} b_n \sin \omega(t - x/c_o) \tag{2.34a}$$

$$b_n = (-1)^{n+1} \frac{2}{n\sigma} J_n(n\sigma) \tag{2.34b}$$

$$\sigma = x/x_c \tag{2.34c}$$

$J_n(\,)$ is the Bessel function of order n.

Beyond the shock formation distance, Blackstock[1] gives the attenuation, α_s, of the fundamental as

$$\alpha_s = (\sigma + 1)/2 \tag{2.35}$$

The amplitudes of the harmonics in this region have not been computed in detail. However, for distances considerably in excess of the shock formation distance, the wave may be assumed to be a sawtooth.

The Fourier series for a sawtooth wave is:

$$p = p_{mx} \sum_{n=1}^{\infty} b_{sn} \sin \omega(t-x/c_o) \tag{2.36a}$$

$$b_{sn} = (-1)^{n+1}\ 1/n \tag{2.36b}$$

Combining these last three equations, Eq. (2.34) for $x/x_c < 1$, Eq. (2.35) for $x/x_c > 2$, and Eq. (2.36) for $x/x_c \gg 1$ ($x/x_c > 5$ say), a plot of the amplitudes of the first four harmonics is obtained and shown in Fig. 2.3.

The solid lines show the region in which formulae are valid, the dotted lines indicate estimated interpolations.

Some caution is needed in the region $x/x_c \gg 1$. Formula (2.35) applies only in the region $\alpha x = 0$. For finite attenuation, the results of Blackstock's computer program are needed. Values are indicated by dashed lines in Fig. 2.3 for various values of αx_c for the fundamental only. Again, from Eq. (2.33) αx is quite small for all cases of interest. The solid lines in Fig. 2.3 are, therefore, reliable within the limits of the most sophisticated computations available.

It should be remembered that the theoretical treatments consider only the classical attenuation. The presence of water vapor in the air introduces additional absorption. This will attenuate the distortion products more than predicted by the classical derivation. This will make αx_c somewhat larger and a more complicated function of frequency.

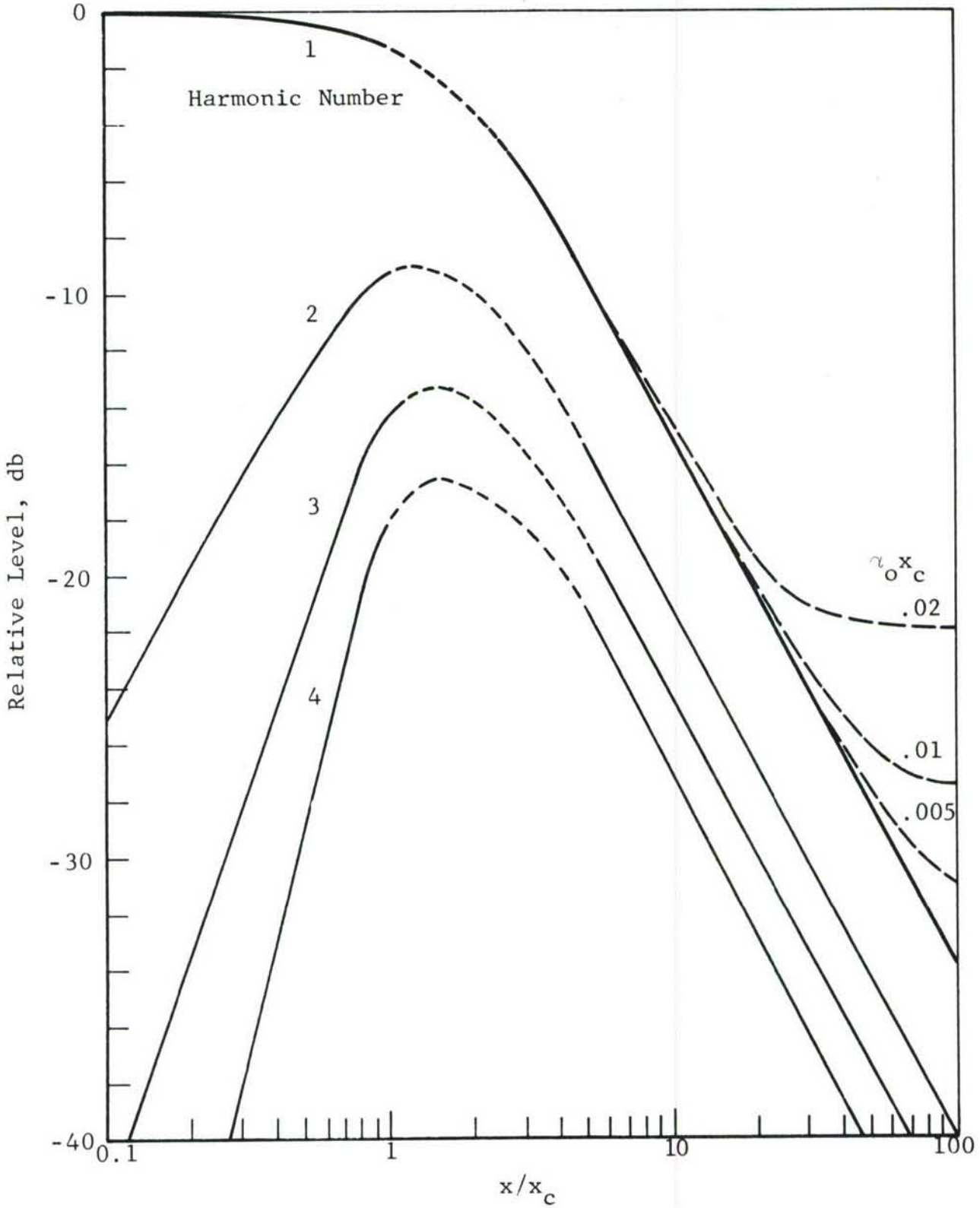

Fig. 2.3. Growth of Harmonics and Attenuation of Plane Waves Due to Finite Amplitude Effects.

2.5 NOTE ON NOISE

All preceding sections have dealt with initially simple harmonic pressure fluctuations. It is of interest also to determine the effects of nonlinearities on nonperiodic functions produced by amplitude and frequency modulation of a siren output.

The taped program normally employed to modulate the frequency and amplitude of the sirens is designed to simulate the properties of band limited white noise.

The most significant difference between band limited noise and simple harmonic motion is the probability distribution of the instantaneous amplitude. For true white noise or filtered white noise this is a Gaussian function having a maximum at zero and approaching zero for very large amplitudes. The exact Gaussian function cannot be achieved either by amplification of random generators or by modulating sirens. In both cases there will always be some finite amplitude above which the probability amplitude will drop to zero much more rapidly than the error function. In the case of modulated sirens, this will be the maximum amplitude the sirens are capable of generating with the modulating ports wide open.

Similar limitations are in practice imposed on band limited noise by maximum power handling capabilities of the amplifiers. The waveforms from the sirens may, therefore, be essentially similar to the kind of waveforms generated by electronic means differing from theoretical Gaussian noise in a minor manner in the region of rarely occurring very large amplitudes. All the probability functions have a maximum value for zero amplitude decaying along the familiar bell-shaped curve for large amplitudes.

For sine waves the amplitude probability function is exactly zero beyond the peak amplitude; moreover this probability amplitude increases from a minimum at zero amplitude to a

cusp-shaped highest value at the peak amplitude. Since nonlinear effects will depend on the amount of time spent at large amplitudes and the values of this largest amplitude, there are two opposing factors. For the same root mean square amplitude the noise function will be of small amplitude a much larger percentage of the time than the simple harmonic function. On the other hand considerably higher amplitudes are reached.

It would be an interesting exercise to attempt a computation on the effect of this different amplitude distribution for the two types of functions considered. This has not been done within the time and budget limitations of the current program. Instead, an experimental program was set up to measure the distortion generated by plane-wave band-limited noise signals. The experimental program is described in Section 9.

The growth of the measured "harmonics" resembles the growth of harmonics of pure tones of a different root mean square amplitude as calculated from Eq. (2.34). By means of a curve fitting technique, it is possible to estimate the difference between the root mean square pressure of noise and simple harmonic functions which give rise to the same amount of signal distortion.

The data indicate that in the region tested the occasional very large amplitudes of the noise signal outweigh their rarer occurrence and the same distortion is produced at a lower RMS level of noise than required with pure tones. However, the data are insufficient to predict this difference for other frequencies, RMS sound pressures, or band widths. Further work along this line would evidently be desirable.

3. DISTORTION IN THE HORN

3.1 MODERATE AMPLITUDE--LOW FREQUENCY

The propagation inside the horn of the siren occurs at much higher intensities than elsewhere and nonlinear effects manifest themselves much more strongly in this region.

The computations quoted by Olson[6] carried out by Thuras, Jenkins and O'Neil[7] show that for moderate amplitudes the relative amplitude of the second harmonic p_2 is given in terms of the sound pressure at the throat p_t by:

$$\frac{p_2}{p_1} = \frac{\sqrt{2}}{2} \frac{\gamma + 1}{\gamma} \frac{p_t}{p_o} \frac{1 - e^{-mx/2}}{m} \frac{\omega}{c} \qquad (3.1)$$

where m is the flare constant of an exponential horn. We substitute in this equation the relative areas of the mouth, S_m, and the throat, S_t, of the horn, and replace the flare constant, m, by the horn cut off frequency, $f_c = mc/4\pi$. Further, let us express the relative level of the second harmonic $L_2 - L_1 = 20 \log p_2/p_1$ at the mouth of the horn in terms of the sound pressure level, L_t, re 0.0002 μbar at the throat

$$S_m = S_t e^{mx_o}$$

$$L_t = 20 \log p_t + 74$$

$$p_o \doteq 10^6 \text{ dynes cm}^{-2} \text{ (1 atmosphere)}$$

$$\gamma = 1.4 \; ; \; (\gamma+1)/\gamma = 1.72$$

$$\omega/mc = \omega/2\omega_c = f/2f_c$$

$$L_2 - L_1$$

$$= L_t + 20 \log \frac{\sqrt{2}}{4} \times 1.72 \times 10^6 + \log (1 - \sqrt{S_t/S_m}) + \log \frac{f}{f_c}$$

$$= L_t + \log f/f_c + \log (1 - \sqrt{S_t/S_m}) - 198 \qquad (3.2)$$

This function is plotted for $S_t \ll S_m$ in Fig. 3.1.

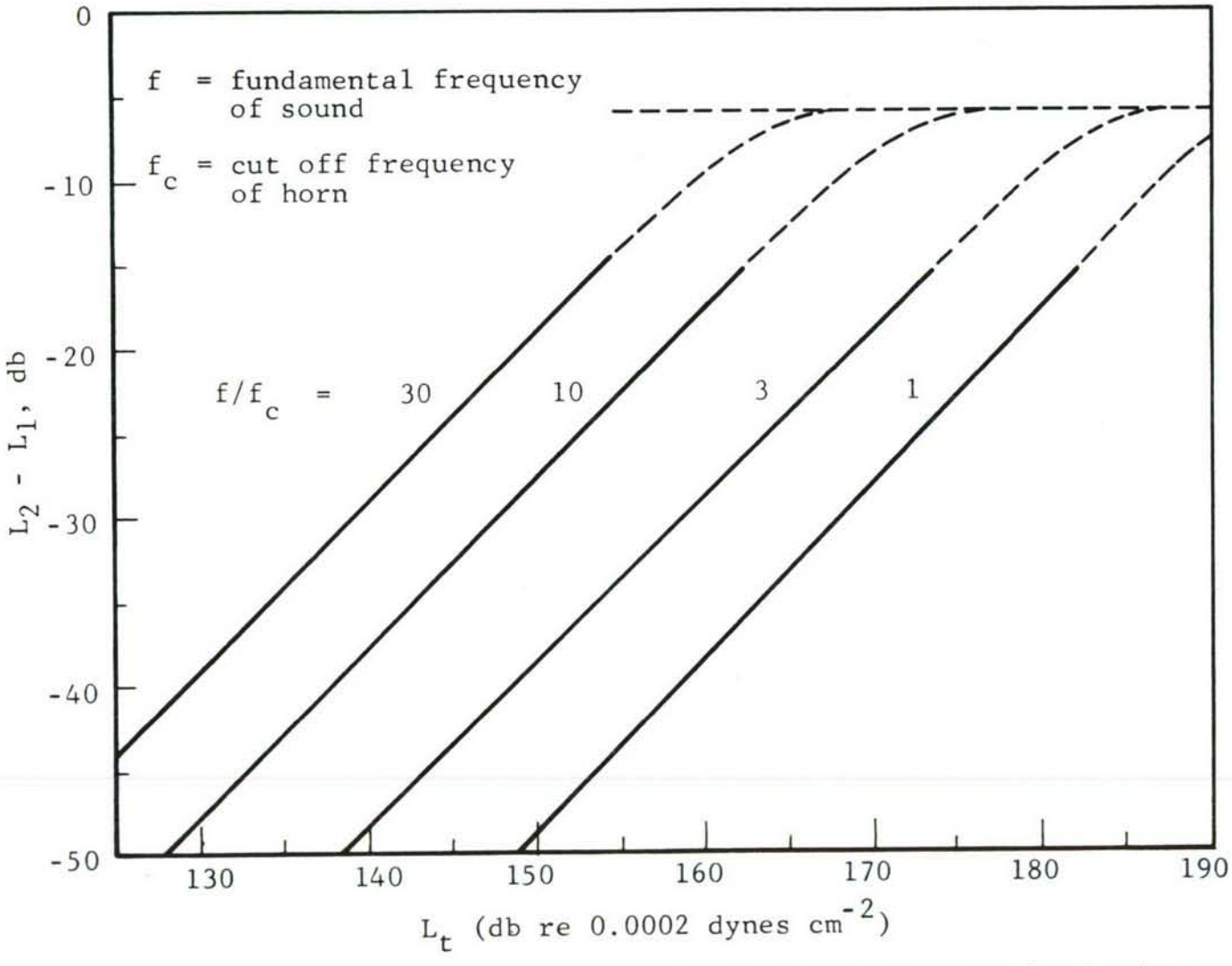

Fig. 3.1. Level of Second Harmonic (L_2) Relative to the Fundamental (L_1) as a Function of the Sound Pressure Level (L_t) in the Throat of the Horn. The parameter is the ratio of the frequency, f, of the sound, to the horn cutoff frequency, f_c.

The derivation assumes that the particle velocity is small (though not as small as for the very small linear theory). Experimental confirmation of the theory is presented for moderate amplitudes.[7] The validity may be expected to be reasonably good up to $L_2 - L_1 \simeq -15$ db.

3.2 LARGER AMPLITUDES--SHOCK WAVES

As the distortion increases, a shock wave forms eventually and once a sawtooth wave form has been established, this wave form retains a reasonably constant shape. The Fourier transform of a sawtooth wave form yields a series of sine functions

$$(-1)^{n+1} \sum_{n=1}^{\infty} \frac{1}{n} \sin n\omega t \qquad (3.3)$$

The amplitude of the second harmonic will be one half the amplitude of the fundamental. On a sound pressure level scale, the second harmonic will be 6 db below the fundamental. The levels of the first ten harmonics with respect to the fundamental are given in Table 3.1.

TABLE 3.1

LEVEL OF HARMONICS IN A SAWTOOTH WAVE

number of harmonic	1	2	3	4	5	6	7	8	9	10
relative level, db	0	-6	-9.5	-12	-14	-16	-17	-18	-19	-20

The interpolation between the level of the second harmonic for a fully developed sawtooth wave form and the moderate amplitude for which theoretical derivations have been verified is shown as a dotted line in Fig. 3.1. The solid lines indicate the levels of second harmonic distortion computed to the extent to which the theory is valid. The parameter on each line gives the

value of the fundamental frequency with respect to the cut off frequency. The maximum value of the peak sound pressure in the throat of the horn for pure sinusoidal excitation is one atmosphere (assuming a one atmosphere mean pressure). The maximum RMS pressure is, therefore, $1/\sqrt{2}$ atmosphere. Maximum possible sinusoidal sound pressure level is, therefore, 20 log (0.713×10^6/ 0.0002) = 191 db. Neglecting losses, the intensity at the mouth is the product of the intensity at the throat and the area ratio:

$$p_m^2 = p_t^2 \, S_m/S_t \, .$$

Expressed in sound pressure level notation

$$L_m - L_s = 10 \log S_m/S_t \, . \qquad (3.4)$$

The throat levels shown on the abscissa of Fig. 3.1 may be converted to sound pressure levels measured at the mouth by subtracting 10 log (S_m/S_t). This formula is valid in the region where distortion is not very severe (second harmonic below about -15 db). Strong distortion products transfer an appreciable amount of energy from the fundamental to the harmonics so that in the regions shown by dotted lines on the curve the corresponding sound pressure level at the mouth will be somewhat lower than computed from the area ratio relation, Eq. (3.4).

The sound pressure levels at which shock waves form was given in Table 2.1. It may be noted that these levels intersect the extrapolated low level distortion curves in Fig. 3.1 at the level $L_2 - L_1 = -6$ db. Thus, there is an additional point in the extrapolation region which lends confidence to the validity of the extrapolation.

Further study of Fig. 3.1 reveals that if distortion is to be minimized, horns must be used near their cut off frequency. Experimentally it has been determined that the distortion in the present sirens is negligible at 300 Hz at full output, but quite severe with pronounced shock formation at 1,000 Hz.

3.3 UTILIZATION OF FACILITY

The nonlinear effects of the propagation of high intensity sound waves may be either reduced by siren redesign or taken into account by computation and calibration over a wide range of sound pressure levels.

3.3.1 Facility Modifications

A redesign of some of the horns and operation of each siren within a more limited frequency range will minimize distortion. Thus, low frequency horns would be used for generating low frequencies only. High frequency sounds would be generated only by the horns specifically designed for that region. The present location of the stator motors limits the design flexibility in this direction within budget limitations.

At any rate, caution must be exercised in replacing present siren horns with horns having a lower cut off in order to generate intense sounds at lower frequencies. A 50 Hz horn operating at 250 Hz will generate as much distortion as a 200 Hz horn operating at 1 kHz. In other words, if some horns are to be replaced with horns having an extended low frequency range, this replacement should be limited to the minimum number necessary.

3.3.2 Compensation for Nonlinear Effects

The present system may be accepted as it is with the generation of harmonics at moderate and high frequencies. Some of the sound power generated will be diverted to harmonics. If this is taken into account, there will be no great loss except that at the highest power levels, performance cannot be extrapolated from measurements at low levels.

4. PROPAGATION OF SPHERICAL WAVES

In the infinitesimal sound theory a useful approximation of a real sound source is frequently the spherical source. This approximation is suitable when the physical dimensions of the source are small relative to the wavelength of sound and/or distances from the source are moderately large relative to wavelength. The region in which spherical spreading is a good approximation was given in Section 2, last line of Table 2.1. If many adjacent sirens operate synchronously, the plane wave region extends proportionately further into the room. Even then spherical spreading is the predominant propagation mode over most of the room.

Analytic models approximating sources of this type have not been incorporated into the problem of propagation of finite amplitude waves. To do so requires the statement of the fundamental differential equations in an appropriate coordinate system and the development of an analytic statement of the boundary conditions appropriate to the sound source and the boundaries of its environment. This has been done for a piston radiating plane progressive waves, and, also, to a limited extent, for spherical sources. These two cases represent, in a sense, limiting cases between which actual sources like the sirens will be expected to fall. The plane wave case represents that extreme wherein loss of intensity in the wave occurs only because of loss to the medium.

4.1 APPLICATION OF THE COMPUTATIONS BY LAIRD AND ACKERMAN TO THE SONIC FATIGUE FACILITY

One approach to the analytic treatment of the propagation of spherical waves of finite amplitude is the paper by Laird and Ackerman.[8] They begin with the usual equations of continuity, motion, and the adiabatic equation of state for a perfect gas in the Eulerian formulation. With the additional assumption of spherical symmetry about the origin, these equations can be stated as:

$$\frac{\partial \rho}{\partial t} + U \frac{\partial \rho}{\partial r} + \rho \frac{\partial U}{\partial r} + \frac{2U\rho}{r} = 0 \qquad (4.1)$$

$$\rho \frac{\partial U}{\partial t} + \rho U \frac{\partial U}{\partial r} + \frac{\partial \rho}{\partial r} = 0 \qquad (4.2)$$

$$\frac{p}{p_o} = \left(\frac{\rho}{\rho_o}\right)^{\gamma} \qquad (4.3)$$

where ρ = density, p = pressure, and U = particle velocity.

The assumption that the gas is non-viscous, non-heat conducting, and non-heat radiating is a common one in the literature; and it is generally assumed that the approximation is satisfactory during that regime in wave propagation before shock waves begin to form.

After several transformations of coordinates, including a normalization, Eqs. (4.1) and (4.2) become

$$\frac{2}{\gamma-1} \frac{\partial S}{\partial \theta} + \frac{2}{\gamma-1} v \frac{\partial S}{\partial x} + (1+S) \frac{\partial v}{\partial x} + \frac{2v(1+S)}{x} = 0 \qquad (4.4)$$

$$\frac{\partial v}{\partial \theta} + v \frac{\partial v}{\partial w} + \frac{2}{\gamma-1} (1+S) \frac{\partial S}{\partial w} = 0 \qquad (4.5)$$

where $v = U/c_o$

$S = (c-c_o)/c_o$

$w = (2\pi/\lambda_o)\, r$

$\theta = 2\pi ft$

f = frequency

λ_o = wavelength of sound in the limit of infinitesimal amplitude

$c = \sqrt{\gamma p/\rho}$ = velocity of sound

$c_o = \sqrt{\gamma p_o/\rho_o}$ = undisturbed speed of sound

Boundary conditions are specified in terms of particle velocity at the surface of a pulsating spherical source with equilibrium radius r_o, in the form

$$U_\rho = U(r_o + \xi_\rho) = U_m \exp j(2\pi ft - \phi) \tag{4.6}$$

$$\xi_\rho = -\frac{1}{2\pi f} U_m \exp j(2\pi ft - \phi) \tag{4.7}$$

where U_m is velocity amplitude of the source and ϕ is an arbitrary phase angle. We note that the boundary conditions do not give the particle velocity at a fixed radius r_o but at a variable radius $r_o + \xi_\rho$ where ξ_ρ is the displacement of the surface of the sphere from equilibrium at time, t.

In normalized coordinates, Eqs. (4.6) and (4.7) are

$$v_\rho = v(w_o + K_\rho, y) = v_m \exp j(\theta - \phi) \tag{4.8}$$

$$K_\rho = -jv_m \exp j(\theta - \phi) \tag{4.9}$$

where $v_\rho = U_\rho / c_o$. Since this formulation gives particle velocity at time t at a variable radius $r_o + \xi_\rho$, it is difficult to apply the boundary conditions in order to obtain a specific solution. This is overcome by expanding particle velocity, v_ρ, in a Taylor's series in terms of particle velocity at radius r_o. That is, we obtain an approximation to what the particle velocity as a function of time must be at r_o to produce the given particle velocity at $r_o + \xi_\rho$ at the same time.

Laird and Ackerman solve the equations by a perturbation method out to the second order approximation. The limiting assumptions made in this procedure include the condition that the source circumference shall not be significantly smaller than one wavelength, i.e., $w_o \gg 1$. Since the horn opening to the sirens is of the order of 1 ft in radius, it seems reasonable to assume that this condition will be met down to frequencies of 200 Hz (wavelength approximately 5.65 ft). The total solution out to second order has the form

$$v(w,\theta) = \underline{A}\Psi_1^{(1)} \exp\, j(\theta-w) + \Psi_0^{(2)} + \Psi_2^{(2)} \exp\, j2(\theta-w) \qquad (4.10)$$

$$S(w,\theta) = \frac{\gamma-1}{2}\left[\underline{A}\sigma_1^{(1)} \exp\, j(\theta-w) + \sigma_0^{(2)} + \sigma_2^{(2)} \exp\, j2(\theta-w)\right] \qquad (4.11)$$

where $\underline{A} = v_m \dfrac{w_o^2}{(w_o^2+1)^{1/2}}$

v_m = normalized particle velocity amplitude at source

$$\Psi_1^{(1)} = \frac{1}{w} - j\frac{1}{w^2} \quad , \quad \sigma_1^{(1)} = \frac{1}{w}$$

$$\Psi_0^{(2)} = \frac{1}{2w^2}$$

$$\Psi_2^{(2)} = (B_2^{(2)} + F_{20}^{(2)})\,\Psi_{20} + F_{21}^{(2)}\Psi_{21}$$

$$\sigma_0^{(2)} = -\frac{\gamma+1}{8}\,\frac{1}{w^2} - \frac{1}{4w^4}$$

$$\sigma_2^{(2)} = \left[B_2^{(2)} + F_{20}^{(2)} - F_{21}^{(2)} \exp(j4w)\right]\frac{1}{w} - \frac{j}{4}\left[\frac{j}{w^2} + \frac{2}{w^3} - \frac{j}{w^4} + \frac{j(\gamma-1)}{2w}\right]$$

$$B_2^{(2)} = \frac{2}{2-jw_o}\,\frac{1}{2}\left(j + \frac{1}{w_o}\right)\frac{\partial \Psi_1^{(1)}}{\partial w}(w_o) - \left(1 + \frac{j}{2w_o}\right) F_{21}^{(2)}(w_o) \exp\, j4w_o$$

$$F_{20}^{(2)} = -\int_{w_o}^{w} \frac{\Psi_{21}}{\Delta_2}\, v_2^{(2)}\, dw \quad ; \quad F_{21}^{(2)} = \int_{\infty}^{x} \frac{\Psi_{20}}{\Delta_2}\, v_2^{(2)}\, dw$$

$$\Delta_2 = j\frac{4}{w^2} \exp\,(j4w) \quad ; \quad \Psi_{20} = \frac{1}{w} - \frac{j}{2w^2}$$

$$\Psi_{21} = \left[\frac{1}{w} + \frac{j}{2w^2}\right] \exp\,(j4w)$$

$$v_2^{(2)} = -j4\left[-\frac{\gamma-1}{4}\,\frac{\partial \sigma_1^{(1)}}{\partial w}\,\sigma_1^{(1)} - \frac{1}{2}\,\frac{\partial \Psi_1^{(1)}}{\partial w}\,\Psi_1^{(1)}\right]$$

The actual solutions are to be the real part of these complex quantities. A computer program was used[8] to obtain numerical results in a reasonable time.

Expanding the perfect gas law into a Taylor series provides an analytic expression for pressure, p, in terms of the solutions for S, the normalized local velocity of sound. Substituting in the solution for S up to second order gives

$$\frac{p}{p_o} = \gamma \underline{A} \frac{1}{w} \exp j(\theta - w) + \gamma \underline{A}^2 \left[B_2^{(2)} + \frac{j(\gamma+1)}{4} \log_e \frac{w}{w_o} \right] \frac{1}{w} \exp j2(\theta - 2) \tag{4.12}$$

The computer calculation gave v, S, and p as functions of normalized distance, $w = (2\pi/\lambda_o)r$ and $v_m = U_m/c_o$. The following tables give the range of these parameters of interest to the Sonic Fatigue Facility program.

TABLE 4.1

NORMALIZING FACTOR VERSUS FREQUENCY

Frequency cps	$\lambda_o/2\pi$ ($r = \lambda_o/2\pi w$)	w_o ($r_o \cong 1$ ft)
200	0.908	1.10
500	0.363	2.75
1000	0.182	5.50
2000	0.091	11.00

TABLE 4.2

NORMALIZED VELOCITY AMPLITUDE VS. SPL

Sound Pressure Level re 0.0002 μbar	$v_m = U_m/c_o$
114	10^{-4}
134	10^{-3}
154	10^{-2}
174	10^{-1}

The computer program used the parametric values of $w_o = 0.2066$, $w_o = 1.0$, and $w_o = 5.0$; and $v_m = 0.05$, $v_m = 0.1$, $v_m = 0.2$, and $v_m = 0.4$. Of these values, $w_o = 1.0$ and $w_o = 5.0$ together with $v_m = 0.05$ are of interest for our case.

This conventional perturbation solution fails to converge at large distances from the source. Therefore, for large values of w, a perturbation solution was developed based on the characteristic equations associated with the basic system of differential equations, Eqs. (4.1), (4.2), and (4.3). The procedure is based on that discussed by Lin.[9] The solution was carried through the second order, but only the first order solution was considered in discussing quantitative results. When the amplitude is low enough $s+v \ll 1$, this perturbation of characteristic equations solution can be used to describe the formation of the shock fronts, their growth and decay. When the amplitude is high near the source but is appreciably diminished by spherical divergence before shocks are formed, it is convenient to use the conventional perturbation solution carried to second or higher order near the source out to some intermediate distance where the amplitude is lower and then to use the first order characteristic perturbation solution for greater distances.

This was done in the computer program by Laird and Ackerman. In Figs. 4.1 and 4.2 we have replotted their results for two cases applicable to the Sonic Fatigue Facility.

In Fig. 4.1, $w_o = (2\pi/\lambda_o)r_o$ was chosen to be 1.0. This corresponds to a frequency of 180 Hz if r_o, the radius of the source, is taken as 1 ft. $v_m = U_m/c_o$ was selected as 0.1 about 174 db SPL. The plot of sound pressure level versus distance for the fundamental falls closely upon the curve for pure spherical spreading, i.e., 6 db per doubled distance. The second harmonic appears prominently at only 1 ft from the source, but decays rapidly. The calculation of the value of the normalized distance at which the shock wave begins to develop, w_{sh}, gives a value $> 10^3$ or approximately 1,000 ft. The expression for w_{sh} is based on the characteristic perturbation solution

$$w_{sh} = w_o \exp\left[\frac{2}{\gamma+1}\,\frac{1}{v_m w_o}\,\frac{(1+w_o^2)^{1/2}}{w_o}\right] \qquad (4.13)$$

It has been assumed that the source is sufficiently weak so that the first order perturbation in the characteristics may be used to describe the whole field and w_o is of the order of magnitude of 1.

The calculations indicate that for frequencies at the lower end of the spectrum, spherical divergence would preclude the formation of shock waves within the Sonic Fatigue Facility due to propagation in the air of the room. This is true for even the very highest sound pressure levels contemplated. The presence of higher harmonics in the sound field at these frequencies would be due to their generation inside the sirens themselves. In other words, since spherical divergence characterizes the sound field at low frequencies, we cannot expect the generation and growth of the higher harmonics.

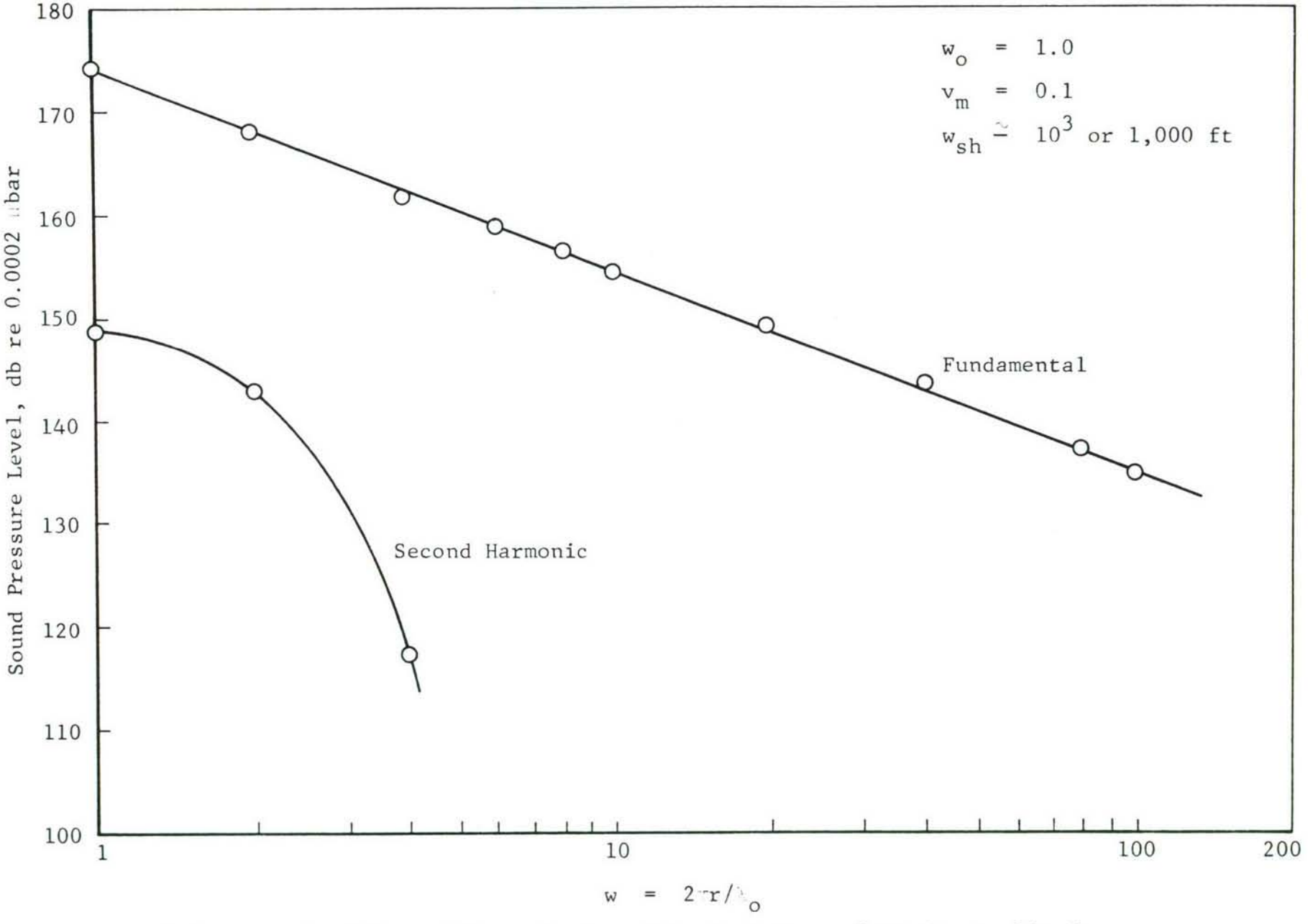

Fig. 4.1. Growth of Second Harmonic in a Spherical Wave of Finite Amplitude.

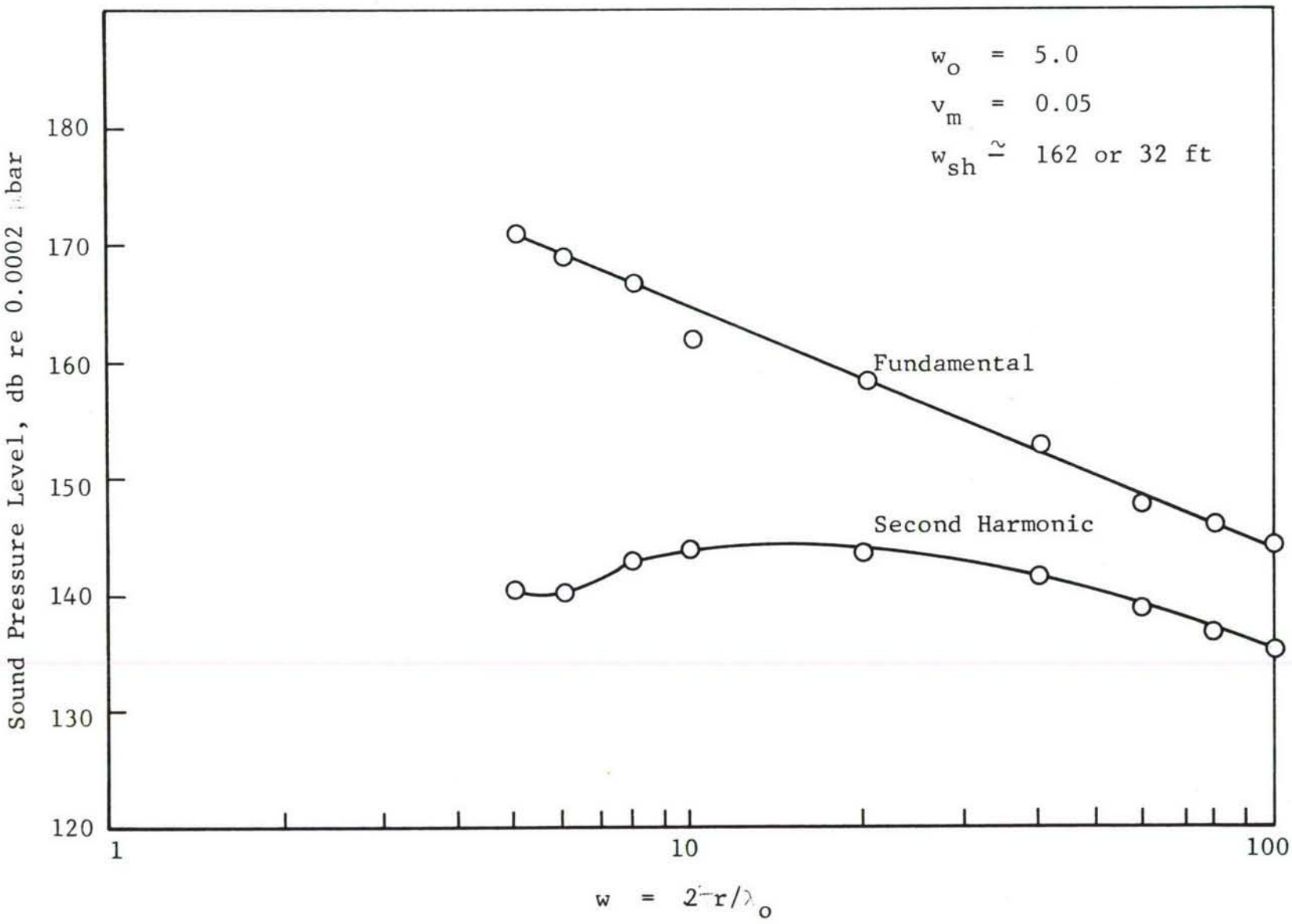

Fig. 4.2. Growth of Second Harmonic in a Spherical Wave of Finite Amplitude.

Figure 4.2 displays the results of the computer program for a choice of $w_o = 5.0$ and $v_m = 0.05$. A choice of $w_o = 5$ corresponds to a frequency of about 1,100 cps if r_o is chosen as 1 ft. The second harmonic grows to a significant component of the signal.

4.2 APPLICATION OF RECENT RUSSIAN LITERATURE TO THE SONIC FATIGUE FACILITY

A more recent treatment of the propagation of finite amplitude spherical waves is that of Naugol'nykh, Soluyan, and Khoblov.[10] This paper represents an attempt to include consideration of viscosity and thermal conductivity of the medium. To do this the Navier-Stokes equation is formulated in the form

$$\rho \left[\frac{\partial U}{\partial t} + U \frac{\partial U}{\partial r} \right] = \rho - \frac{\partial p}{\partial r} + b \left[\frac{1}{r} \frac{\partial^2 (rU)}{\partial r^2} - \frac{2}{r^2} U \right] ; \qquad (4.14)$$

where $b = 4/3\ \eta + \eta' + k \left[\frac{1}{c_v} - \frac{1}{c_p} \right]$

represents the results of combining the viscosity terms in the Navier-Stokes equations and the heat terms in the equation of state taking into account the fact that the process is non-adiabatic. The total system of equations to be solved is completed by the equation of continuity and the approximate equation of state.

$$\frac{\partial \rho}{\partial t} + U \frac{\partial \rho}{\partial r} + \rho \frac{\partial U}{\partial r} + \frac{2\rho U}{r} = 0 \qquad (4.15)$$

$$p = p_o + c^2 (\rho - \rho_o) + \frac{\gamma - 1}{2} \frac{\rho_o}{c_o^2} (\rho - \rho_o)^2 \qquad (4.16)$$

A series of transformations and approximations leads to the final differential equation to be solved

$$\frac{\partial U}{\partial r} + \frac{U}{r} - AU\frac{\partial U}{\partial t} = \delta\frac{\partial^2 U}{\partial \tau^2} \qquad (4.17)$$

where $A = \frac{\gamma+1}{2c_o^2}$; $\delta = \frac{b}{2\rho_o c_o^3}$; $\tau = t - \frac{r}{c_o}$

For the case of air, values for these constants are:

$$b \cong 9.12 \times 10^{-6} \frac{\text{Newton sec}}{m^2}$$

$$A = 9.90 \times 10^{-6} \frac{\text{sec}^2}{\text{meters}^2}$$

$$\delta = 9.22 \times 10^{-14} \frac{\text{Newton sec}^4}{\text{meter}^2\ \text{kgm}}$$

Equation (4.17) is solved in the case of large values of the reciprocal dissipation factor, R, i.e.,

$$\Gamma = \frac{AU_o}{2\omega\delta} \gg 1 \quad , \text{ i.e., } \quad \delta \cong 0 \ . \qquad (4.18)$$

In our case

$$\Gamma = \frac{(9.90 \times 10^{-6})(3.0)}{4\pi f\ (9.22) \times 10^{-14}} \cong 2.56 \times 10^8 \times \frac{1}{f}$$

where f is frequency. For all frequencies of interest $f < 10{,}000$ Hz, $R \gg 1$, and this solution should apply. In Eq. (4.17) we can, therefore, drop the term on the right side of the equality sign. The resulting equation together with the boundary conditions $U = U_o \sin(\omega t - kr_o)$ at the surface of the pulsating medium $r = r_o$, leads to the solution

$$\omega\tau = \arcsin \epsilon - A\omega U_o r_o \log_e \frac{r}{r_o}\epsilon \qquad (4.19)$$

where $\epsilon = \frac{Ur}{U_o r_o}$

This solution describes the propagation of the wave prior to the formation of the shock wave where dissipative process plays no substantial role, $\Gamma \gg 1$. Except for the second term, $GU_o \omega r_o \log_e (r/r_o)$, this solution would be a spherically diverging sinusoidal wave. The term $X = G\omega U_o r_o \log_e (r/r_o)$ results in a progressive steeping of the wave front. At any instant, t, this factor increases logarithmically with r. If X is less than 1 this distortion is modest for $X < 1$, strong when X is comparable to 1, and at $X > 1$, $\omega\tau$ becomes multivalued. The condition that X = 1 can be used as a criterion to define the point, r, where the shock wave begins. This leads to

$$\frac{r_1}{r_o} = \exp \frac{1}{kr_o \dfrac{(\gamma+1)U_o}{2c_o}} = \exp \frac{2}{\gamma+1} \frac{1}{w_o v_{mo}} \qquad (4.20)$$

which is equivalent to Eq. (4.13) of the earlier theory under the approximation that w_o is about 1.

As an example: f = 3000 Hz and $v_m = U_o/c_o = 0.05$, $r_o = 0.304$ m = 30.4 cm = 1 ft, r_1 becomes 2.7 r_o, i.e., 2.7 ft. The plane wave shock formation distance at this intensity (171 db re 0.0002 dynes cm^{-2}) from Table 2.1 would be 0.7 ft. This shows the extent to which spherical spreading by reducing intensity also reduces the distortion.*

The two theoretical treatments give essentially the same results except that Laird [8], expresses his results for pressure in a form that provides estimates of the pressure

---

*Naugol'nykh, et al, state that their assumption of negligible attenuation ($R \gg 1$) is valid only for the region in which distances are not very large compared with r_o. The formula is, therefore, not valid for low frequencies or moderate amplitude when shock formation distances would become very large.

levels for each harmonic as a function of radial distance from the source while Naugol'nykh[10] presents a much simpler relationship from which the wave form may be obtained as a function of distance. Laird's procedure requires, however, a computer program (already developed and used) to obtain results for a specific value of the parameters. This is especially true if we wish information about harmonics higher than the second.

5. FINITE AMPLITUDE PLANE ACOUSTIC WAVES

The most general differential equations involving wave propagation in a gaseous medium[11] are quite complex mathematically and at the present time are unsolvable. However, by making suitable approximations these differential equations may be linearized and the resulting simplified equations can be solved to yield solutions applicable to "small" signal propagation.

With the advent of more powerful acoustic sources, many of the approximations made in obtaining the "small signal equations" cannot be used if a useful analysis of the propagation is to be made. A consequence of this limitation is that the differential equations of wave propagation become nonlinear. Two methods of approach have been used in an attempt to solve the nonlinear problem. The first and most common method[11,12] is that utilizing perturbation techniques to obtain solutions. A disadvantage of this method is that it is relatively weak and is tedious to use in practice. The second method is that of transforming the equations into a nonlinear equation whose solution is known. Blackstock[1,14] shows how the nonlinear plane wave equations may be transformed into an equation called Burger's equation whose solution for initial value problems is known. The dependent variable is particle velocity. It is this method which will be used in this discussion.

An approximate form of the equations of motion in a thermoviscous medium is given by Blackstock as:

$$c_o^2 U_x - \beta c_o U U_{t'} = \frac{1}{2} \nu \left[Y + (\gamma-1)/P_r \right] U_{t't'} = \nu' U_{t't'} \qquad (5.1)$$

where x is distance, $t' = t - x/c_o$, t is time, c_o is small signal sound speed in the absence of dissipation, ν iv kinematic viscosity, $Y = 2 + \eta'/\eta$ is the viscosity number, η and η' are the shear and dilational viscosity coefficients respectively, γ is the ratio of specific heats, and P_r is the Prandtl number.

The quantity β is given by $1/2(\gamma+1)$ for perfect gases. Dividing through by c_o^3 and letting $z = t'/A$, one obtains the equation

$$U_x - UU_z = CU_{zz} \tag{5.2}$$

where

$$A = \beta/c_o^2$$

$$C = \frac{c_o \nu'}{2\beta^2}$$

Using the transformation

$$U = 2C\,[\text{low } \zeta]_z \tag{5.3}$$

the equation reduces to

$$\zeta_x = C\zeta_{zz} \tag{5.4}$$

where it has been assumed that $\zeta \neq 0$. Making a further change of variables $x \rightarrow y = xc$, one obtains the equation

$$\zeta_y = \zeta_{zz} \tag{5.5}$$

which has the initial-value-problem solution[15]

$$\zeta(y,z) = \frac{1}{\sqrt{4\pi}} \int_{-\infty}^{\infty} \frac{\phi(p)}{(y)^{1/2}} \exp \frac{-(z-p)^2}{4y}\, dp \quad \text{for} \quad y > 0 \tag{5.6}$$

where

$$\phi(p) = \zeta(0,p) \tag{5.7}$$

In the case at hand

$$\zeta(0,p) = \exp \frac{1}{2C} \int_0^p U(0,m)\, dm \tag{5.8}$$

This derivation was included here as the basis for both Section 6 and Section 7.

6. SUPERPOSITION OF FINITE AMPLITUDE WAVES

Let us now consider the case where two plane progressive waves which are sinusoidal at the origin are superimposed throughout space. Thus,

$$\left.\begin{aligned} U(o,m) &= U_1 \sin(\omega_1 Am) + U_2 \sin(\omega_2 Am + \delta)\ ;\ t > 0 \\ U(o,m) &= 0\ ;\ t < 0 \end{aligned}\right\} \qquad (6.1)$$

at the initial point of superposition. Evaluating the integral, Eq. (5.3), we obtain the result that

$$\zeta(0,p) = \overline{B} \exp \frac{-U_1}{2C\omega_1 A} \cos(\omega_1 Ap) - \frac{U_2}{2C\omega_2 A} \cos(\omega_2 Ap + \delta) \qquad (6.2)$$

where

$$\overline{B} = \exp\left[\frac{U_1}{2C\omega_1 A} + \frac{U_2 \cos\delta}{2C\omega_2 A}\right] \qquad (6.3)$$

Thus, from Eq. (5.6)

$$\zeta(y,z) = \frac{\overline{B}}{\sqrt{4\pi y}} \int_0^\infty \exp\left[\frac{-U_1}{2C\omega_1 A} \cos(\omega_1 Ap) + \frac{-U_2}{2C\omega_2 A} \cos(\omega_2 Ap + \delta) - \frac{(z-p)^2}{4y}\right] dp +$$

$$\frac{\overline{B}}{\sqrt{4\pi y}} \int_{-\infty}^0 \exp\left[\frac{-U_1}{2C\omega_1 A} \cos(\omega_1 Ap) + \frac{-U_2}{2C\omega_2 A} \cos(\omega_2 Ap + \delta) - \frac{(z-p)^2}{4y}\right] dp \qquad (6.4)$$

The second integral will vanish in the steady state, $z \to \infty$. Making use of the relations[16]

$$e^{-z\cos\theta} = \sum_{n=0}^{\infty} (-1)^n I_n(z)\, \epsilon_n \cos n\theta$$

$$\epsilon_n = \left.\begin{array}{l} 1 \text{ if } n = 0 \\ 2 \text{ if } n \geq 1 \end{array}\right\} n, \text{ an integer}$$

$I_n(z)$ = Modified Bessel Function

we obtain

$$\zeta(y,z) = \frac{\overline{B}}{\sqrt{4\pi y}} \int_0^\infty \left[\left(\sum_{R=0}^{\infty} (-1)^k \epsilon_k I_k \frac{U_1}{2C\omega_1 A} \cos(k\omega_1 Ap) \right) \right.$$
$$\left. x \left(\sum_{\ell=0}^{\infty} (-1) \epsilon_\ell I_\ell \frac{U_2}{2C\omega_2 A} \cos(\ell\omega_2 Ap + \ell\delta) \right) \exp \frac{-(z-p)^2}{4y} \right] dp \qquad (6.5)$$

$$\zeta(y,z) = \frac{\overline{B}}{\sqrt{4\pi y}} \sum_{k=0}^{\infty} \sum_{\ell=0}^{\infty} A(k,\ell) \int_0^\infty \cos(k\omega_1 Ap) \cos(\ell\omega_2 Ap + \ell\delta)$$
$$\cdot \exp\left(\frac{-(z-p)^2}{4y}\right) dp \qquad (6.6)$$

where

$$A(k,\ell) = (-1)^{k+\ell} \epsilon_k \epsilon I_k \left(\frac{U_1}{2C\omega_1 A}\right) I_\ell \left(\frac{U_2}{2C\omega_2 A}\right) \qquad (6.7)$$

Making use of the following relations

$$\lim_{z \to \infty} \int_0^\infty \cos(\bar{a}p) \exp \frac{-(z-p)^2}{4y} dp = \sqrt{4\pi y} \cos(\bar{a}z) \exp(-\bar{a}^2 y)$$

$$\lim_{z \to \infty} \int_0^\infty \sin(\bar{b}p) \exp \frac{-(z-p)^2}{4y} dp = \sqrt{4\pi y} \sin(\bar{b}z) \exp(-\bar{b}^2 y)$$

Together with various trigonometric relations, we obtain the value of the integral in Eq. (6.6) for the steady state ($z \to \infty$).

$$I = \lim_{z\to\infty} \int_0^\infty \cos(k\omega_1 Ap) \cos(\ell\omega_2 A_p + \delta\ell) \exp \frac{-(z-p)^2}{4y}\, dp$$

$$= \frac{\sqrt{4\pi y}}{2} \cos[(\ell\omega_2+k\omega_1) Az + \ell\delta] \exp[-(\ell\omega_2+k\omega_1)^2 A^2 y] +$$

$$\cos[(\ell\omega_2-k\omega_1) Az + \delta\ell] \exp[-(\ell\omega_2-k\omega_1)^2 A^2 y] \qquad (6.8)$$

Thus

$$\zeta(y,z) = \frac{\overline{B}}{\sqrt{4\pi y}} \sum_{k=0}^{\infty} \sum_{\ell=0}^{\infty} A(k,\ell)\, I \qquad (6.9)$$

and the particle velocity becomes

$$U(y,z) = 2C\,[\log \zeta]_z \qquad (6.10)$$

where $z = t'/A$ and $y = xC$

In the expanded form, the equation is

$$U = 2C\Bigg(\sum_{k=0}^{\infty} \sum_{\ell=0}^{\infty} (-1)^{k+\ell+1} \epsilon_k \epsilon_\ell I_k(U_1/2C\omega_1 A)\, I_\ell(U_2/2C\omega_2 A)$$

$$(\ell\omega_2+k\omega_1)A \exp[-(\ell\omega_2+k\omega_1)^2 A^2 y] \sin[(\ell\omega_2+k\omega_1)Az+\delta\ell] +$$

$$(\ell\omega_2-k\omega_1)A \exp[-(\ell\omega_2-k\omega_1)^2 A^2 y] \sin[(\ell\omega_2-k\omega_1)Az+\ell\delta]\Bigg)\Bigg(\sum_{k=0}^{\infty}$$

$$\sum_{\ell=0}^{\infty} (-1)^{k+\ell} \epsilon_k \epsilon_\ell I_k(U_1/2C\omega_1 A) I_\ell(U_2/2C\omega_2 A) \Big\{\cos[(\ell\omega_2+k\omega_1)Az+\delta\ell]$$

$$\cdot \exp[-(\ell\omega_2+\omega_1 k)^2 A^2 y] + \cos[(\ell\omega_2-k\omega_1)Az]$$

$$\cdot \exp[-(\ell\omega_2-k\omega_1)^2 A^2 y]\Big\}\Bigg) \qquad (6.11)$$

For the case of a single source, we let U_2 and δ approach zero. Noting that

$$\lim_{U_2\to 0} I_\ell(U_2/2C\omega_2 A) = \begin{cases} 0 \text{ if } \ell \neq 0 \\ 1 \text{ if } \ell = 0 \end{cases}$$

We find that the particle velocity due to a single source can be given as

$$U = 2C \left[\sum_{k=0}^{\infty} (-1)^{k+1} \epsilon_k I_k \, (U_1/2C\omega_1 A) k\omega_1 A \exp(-k^2\omega_1{}^2 A^2 y) \cdot \begin{matrix} \sin(k\omega_1 Az) \\ \cos(k\omega_1 Az) \end{matrix} \right] \Bigg/ \left[\sum_{k=0}^{\infty} (-1)^k \epsilon_k I_k (U_1/2C\omega_1 A) \exp(-k^2\omega_1{}^2 A^2 y) \cdot \begin{matrix} \sin(k\omega_1 Az) \\ \cos(k\omega_1 Az) \end{matrix} \right] \tag{6.12}$$

(It is to be noted that this solution is identical to that given by Blackstock.) The result in Eq. (6.12) may be simplified by noting that for large arguments

$$I_k(z) \sim (e^z/\sqrt{2\pi z}) \left(1 - \frac{4k^2-1}{8z} + \frac{(4k^2-1)(4k^2-9)}{2!\,(8z)^2} - \ldots.\right) \tag{6.13}$$

Blackstock[14] has shown that we need use only the first term of the asymptotic expansion for $I_k(z)$ when y is large. This is so because in the product of the exponential term and the term in $I_k(z)$ in Eq. (6.12) the exponential term dominates the $I_k(z)$ term when y is large, i.e., this product approaches zero as y becomes large. The restriction that y be large means that the solution obtained from Eq. (6.12) by using the first term of the expansion for $I_k(z)$ in Eq. (6.13) will probably not be valid near the source.

Making the substitution for $I_k(z)$ from Eq. (6.13) into Eq. (6.12), we obtain

$$U = 2C \frac{\sum_{k=0}^{\infty} (-1)^{k+1} (\epsilon_R)(k\omega_1 A) \exp[-k^2\omega_1{}^2 A^2 y]}{\sum_{k=0}^{\infty} (-1)^R \epsilon_R \exp[-k^2\omega_1{}^2 A^2 y]} \tag{6.14}$$

The quantity

$$\phi = \sum_{k=0}^{\infty} (-1)^k \epsilon_k \exp(-k^2\omega_1{}^2A^2y) \cos(k\omega_1 z)$$

$$= \theta_4\left[\frac{\omega_1 Az}{2}, \exp(-\omega_1{}^2A^2y)\right] \qquad (6.15)$$

where θ_4 is a theta function.[16] Now

$$\frac{(\theta_4)_U(U,q)}{\theta_4(U,q)} = 4\sum_{n=1}^{\infty} \frac{q^n}{1-q^{2n}} \sin 2nU \quad |q| < 1 \qquad (6.16)$$

We see, therefore, that

$$U(x,t) = 2C \frac{\left[\theta_4\left(\frac{\omega_1 Az}{2}\right), \exp(-\omega_1{}^2A^2y)\right]_z}{\left[\theta_4\left(\frac{\omega_1 Az}{2}\right), \exp(-\omega_1{}^2A^2y)\right]}$$

$$= 2C \frac{[\theta_4(\omega_1 Az/2), \exp(-\omega_1{}^2A^2y)](\omega_1 Az/2)}{[\theta_4(\omega_1 Az/2), \exp(-\omega_1{}^2A^2y)]} \frac{\omega_1 A}{2}$$

or simplifying

$$U(x,t) = 4C\omega_1 \sum_{n=1}^{\infty} \frac{\exp(-\omega_1{}^2A^2yn)}{1 - \exp(-2\omega_1{}^2A^2yn)} \sin(n\omega Az)$$

$$= 2C\omega_1 A \sum_{n=1}^{\infty} \frac{\sin(n\omega_1 Az)}{\sinh(\omega_1{}^2A^2yn)}$$

$$= 2C\omega_1 A \sum_{n=1}^{\infty} \frac{\sin[n\omega_1(t - x/c_o)]}{\sinh(\omega_1{}^2A^2xCn)} \qquad (6.17)$$

7. NORMAL INCIDENCE REFLECTION FROM A HARD WALL UNDER SPECIAL CONDITIONS (NORMAL INCIDENCE)

An approximate solution to the problem of reflection from a wall may be obtained if the following assumptions are made. Let a finite amplitude plane wave source be located at a point x = 0. Let a perfectly reflecting wall be located at a point x = p, far enough from the source so that the attenuation of the primary wave makes possible the linear superposition of two waves in this region (as in the small signal case).

Under the above conditions, the totally reflecting wall may be replaced by an image source satisfying the boundary condition that the sum of the particle velocities due to the primary source and the image source is zero at the position of the wall (x = p). From Eq. (6.12) the primary source may be given as

$$U_I = 2C \left[\sum_{k=0}^{\infty} (-1)^{k+1} \epsilon_k I_k \, (U_1/2C\omega_1 A) \exp\left[-(k\omega_1 A)^2 Cx\right](k\omega_1 A) \cdot \sin\left\{ \frac{k\omega_1 A c_o^{\,2}}{\beta} (t - x/c_o) \right\} \right] \Bigg/ \left[\sum_{k=0}^{\infty} (-1)^k \epsilon_k I_k \, (U_1/2C\omega_1 A) \cdot \exp\left[-(k\omega_1 A)^2 Cx\right] \cos\left\{ \frac{k\omega_1 A c_o^{\,2}}{\beta} (t - x/c_o) \right\} \right] \tag{7.1}$$

where

$$y = xC$$

$$z = \frac{c_o^{\,2}}{\beta} (t - x/c_o)$$

For the image source the particle velocity satisfying the boundary conditions is

$$U_R = 2C \left[\sum_{k=0}^{\infty} (-1)^{k+1} \epsilon_k I_k \, (U_1/2C\omega_1 A) \exp\left[(k\omega_1 A)^2 (x-2p)C\right] \cdot \right.$$

$$\left. (k\omega_1 A) \sin\left(\frac{k\omega_1 A c_o^2}{\beta} \left(\frac{x-2p}{c_o} - t \right) \right) \right] \Bigg/ \left[\sum_{k=0}^{\infty} (-1)^k \epsilon_k I_k (U_1/2C\omega_1 A) \right.$$

$$\left. \exp\left[(k\omega_1 A)^2 (x-2p)C\right] \cos\left(\frac{k\omega_1 A c_o^2}{\beta} \left(\frac{x-2p}{c_o} - t \right) \right) \right] \qquad (7.2)$$

The composite field is thus

$$U_{Total} = U_I + U_R \qquad (7.3)$$

8. AUTOCORRELATION PROPERTIES OF A BAND OF FINITE AMPLITUDE, PLANE WAVE, WHITE NOISE

The autocorrelation function of a signal may be obtained from the following Fourier transform,[22]

$$R(\tau) = \int_0^\infty S(f) \cos 2\pi f\tau \, df = \frac{1}{2\pi} \int_0^\infty S(\omega) \cos(\omega\tau) \, d\omega \quad (8.1)$$

where $R(\tau)$ is the autocorrelation function and $S(f)$ is the power spectral density. To an approximation (which is valid for the sound pressure levels expected in the RTD facility), the sound power in a plane wave is proportional to the square of the sound pressure, where pressure is, in turn, proportional to the particle velocity U. Thus,

$$R(\tau) = \frac{z}{2\pi} \int_0^\infty [U_s(\omega)]^2 \cos(\omega\tau) \, d\omega \quad (8.2)$$

where z = constant $\cong \rho_o c_o$

U_s = RMS particle velocity spectral density

The RMS velocity spectral density for the initially finite amplitude plane wave is,

$$U_s = \lim_{n \to \infty} \left[\frac{1}{n\underline{t}} \int_0^{n\underline{t}} U^2 dt \right]^{1/2}$$

$$= \lim_{n \to \infty} \left[\frac{1}{n\underline{t}} \int_0^{n\underline{t}} \left(2C\omega_1 A \sum_{n=1}^{\infty} \frac{\sin[n\omega_1(t-x/c_o)]}{\sinh(\omega_1^2 A^2 x C n)} \right)^2 dt \right]^{1/2}$$

$$= \sqrt{2}\, C\omega_1 A \left(\sum_{n=1}^{\infty} \frac{1}{\sinh^2(\omega_1^2 A^2 x C n)} \right)^{1/2} \quad (8.3)$$

where $\underline{t}$ is the period $1/f_1$.

For the sinusoidal plane wave the correlation function is

$$R_{\omega_1}(\tau) = \frac{zC^2A^2}{\pi}\int_0^\infty \omega^2 \cos(\omega\tau) \sum_{n=1}^{\infty} \frac{1}{\sinh^2(\omega^2A^2xCn)} \delta(\omega=\omega_1)d\omega$$

$$= \frac{zC^2A^2\omega_1{}^2\cos\omega_1\tau}{\pi} \sum_{n=1}^{\infty} \frac{1}{\sinh^2(\omega_1{}^2A^2xCn)} \qquad (8.4)$$

where $\delta(\omega)$ is the Dirac Delta Function. The correlation coefficient may be determined to be

$$\underline{R}_{\omega_1}(\tau) = R_{\omega_1}(\tau)/R_{\omega_1}(0) = \cos\omega_1\tau \qquad (8.5)$$

For the case of a finite band of noise $\omega_1 < \omega < \omega_2$, Eq. (8.2) becomes

$$R(\tau) = \frac{z}{2\pi}\int_{\omega_1}^{\omega_2} 2C^2\omega^2A^2\cos\omega\tau \left[\sum_{n=1}^{\infty} \frac{1}{\sinh^2(\omega^2A^2xCn)}\right] d\omega$$

$$= \frac{zC^2A^2}{\pi} \sum_{n=1}^{\infty} \int_{\omega_1}^{\omega_2} \frac{\omega^2\cos\omega\tau}{\sinh^2(\omega^2A^2xCn)} d\omega \qquad (8.6)$$

This integral can be evaluated in the following manner. Let

$$I = \int \frac{\omega^2\cos\omega\tau}{\sinh^2(\omega^2\alpha)} d\omega = \int \omega^2(\cos\omega\tau)[\mathrm{CsCh}^2(\omega^2\underline{\alpha})] d\omega \qquad (8.7)$$

where $\underline{\alpha} = A^2xCn$. We may now integrate this integral with respect to the parameter $\underline{\alpha}$.

$$J = I d\underline{\alpha} = \int \omega^2\cos(\omega\tau) \int \mathrm{CsCh}^2(\omega^2\underline{\alpha})\, d\underline{\alpha}d\omega$$

$$= -\int \cos(\omega\tau)\ \mathrm{Ctnh}(\omega^2\underline{\alpha})\, d\omega \qquad (8.8)$$

We may now use the expansion

$$\text{Ctnh}(\omega^2\underline{\alpha}) = \frac{\exp(\omega^2\underline{\alpha}) + \exp(-\omega^2\underline{\alpha})}{\exp(\omega^2\underline{\alpha}) - \exp(-\omega^2\underline{\alpha})}$$

$$= \frac{(1 + e^{-2\omega^2\underline{\alpha}})}{(1 - e^{-2\omega^2\underline{\alpha}})} = 1 + 2\sum_{k=1}^{\infty} \exp(-2k\omega^2\underline{\alpha}) \qquad (8.9)$$

Thus

$$J = -\int \cos(\omega\tau)\left[1 + 2\sum_{k=1}^{\infty} \exp(-2k\omega^2\underline{\alpha})\right] d\omega$$

$$= -\frac{\sin\omega\tau}{\tau} - 2\sum_{k=1}^{\infty}\int \exp(-2k\omega^2\underline{\alpha}) \cos\omega\tau \, d\omega$$

$$= -\frac{\sin\omega\tau}{\tau} - 2\sum_{k=1}^{\infty} \Omega(\underline{\alpha},\gamma) \qquad (8.10)$$

Making use of the fact that

$$\int \exp[-(\underline{\alpha}x^2 + 2bx + C)]\, dx$$

$$= \frac{1}{2}\sqrt{\frac{\pi}{a}} \exp -\frac{b^2 - aC}{a} \text{ erf } \sqrt{a}x + \frac{b}{\sqrt{a}} \qquad (8.11)$$

where the erf term denotes the error function. We see that

$$\Omega(\omega,i) = \text{Re}\int \exp -(2k\omega^2\underline{\alpha} - i\omega\tau)\, d\omega$$

$$= \frac{1}{2}\left(\frac{\pi}{2k\underline{\alpha}}\right)^{1/2} \exp -\frac{\tau^2}{8k\underline{\alpha}} \text{ Re } i \text{ erf}\left(\sqrt{2k\underline{\alpha}}\omega i + \frac{\tau}{2\sqrt{2k\underline{\alpha}}}\right) \qquad (8.12)$$

Making use of the fact that

$$\text{erf}(z) = \frac{2}{\sqrt{\pi}} \sum_{m=0}^{\infty} \frac{(-1)^m z^{2m+1}}{m!\,(2m+1)} \qquad (8.13)$$

and

$$\sqrt{2k\underline{\alpha}}\,\omega i + \frac{\tau}{2\sqrt{2k\underline{\alpha}}} = \left(\frac{\tau^2}{8k\underline{\alpha}} + 2k\underline{\alpha}\omega^2\right)^{1/2} e^{i\theta} \tag{8.14}$$

where $\theta = \tan^{-1}(\tau/2\omega)$. We obtain the results that

$$\Omega = \frac{1}{\sqrt{2k\underline{\alpha}}} \exp - \frac{\tau^2}{8k\underline{\alpha}} \sum_{m=0}^{\infty} \frac{(-1)^{m+1} \left(\tau^2/8k\underline{\alpha}\right) + 2k\underline{\alpha}\omega^2 \Big)^{m+1/2} (\sin\theta)}{m!\ (2m+1)} \tag{8.15}$$

$$J = -\frac{\sin\omega\tau}{\tau} - 2\sum_{k=1}^{\infty} \frac{\exp\left(-\tau^2/8k\underline{\alpha}\right)}{\sqrt{2k\underline{\alpha}}} \cdot \cdot \sum_{m=0}^{\infty} \frac{(-1)^{m+1}\left[\left(\tau^2/8k\underline{\alpha}\right) + 2k\underline{\alpha}\omega^2\right]^{m+1/2} \sin\theta}{m!\ (2m+1)} \tag{8.16}$$

$$I = \frac{\partial J}{\partial \alpha} = -2\sum_{k=1}^{\infty}\sum_{m=0}^{\infty} \left[\frac{(-1)^{m+1}\sin\theta}{m!\ (2m+1)} \exp\left(-\tau^2 8k\underline{\alpha}\right) \cdot \cdot \frac{\left[\left(\tau^2/8k\underline{\alpha}\right) + 2k\underline{\alpha}\omega^2\right]^{m+1/2}}{\sqrt{2k\underline{\alpha}}}\right] \left[\frac{\tau^2}{8k\underline{\alpha}^2} - \frac{1}{2\underline{\alpha}} + \frac{(m+1/2)\left[2k\omega^2 - \left(\tau^2/8k\underline{\alpha}^2\right)\right]}{\left[\left(\tau^2/8k\underline{\alpha}\right) + 2k\underline{\alpha}\omega^2\right]}\right] \tag{8.17}$$

We finally obtain for the correlation function

$$R(\tau) = -\frac{2zC^2A^2}{\pi} \sum_{n=1}^{\infty}\sum_{k=1}^{\infty}\sum_{m=1}^{\infty} \left[I_{m,n,k}(\omega_2) - I_{m,n,k}(\omega_1)\right] \tag{8.18}$$

where $\underline{\alpha} = A^2 x C n$ and $\theta = \arctan \tau/2\omega$ or $\sin\theta = \tau/\sqrt{4\omega^2+\tau^2}$ $\cong \tau/\sqrt{4\omega^2+\tau^2}$ since θ is small. From the definition of

$A = \beta/c_o^2 = 1.2/c_o^2$, $\underline{\alpha} \cong 9.04$ (r/f). From Eq. (8.22) we obtain the autocorrelation coefficient defined as

$$\underline{R(\tau)} = R(\tau)/R(0)$$

In Ref. 17, it was pointed out that the total sound field within the Sonic Fatigue Facility when used in the semi-anechoic mode with a reflecting floor could be predicted in terms of the known autocorrelation coefficient of the sound signal and the radiative characteristic of the sound field. For the case of a simple source radiating into infinite half space over a hard reflecting surface, the expression giving the RMS pressure at any field point is

$$\overline{\underline{P}^2} = \overline{\underline{P}_1^2} + \overline{\underline{P}_2^2} + 2\underline{R}(\tau)\,[\overline{\underline{P}_1^2}\;\overline{\underline{P}_2^2}]^{1/2} \qquad (8.23)$$

In the far field where $\overline{\underline{P}_1^2} \cong \overline{\underline{P}_2^2}$, it is seen that $\overline{\underline{P}^2}$ depends upon $\underline{R}(\tau)$ and the distance from the source.

For the infinitesimal amplitude case this resulted in a far field with a characteristic interference pattern. For narrow bands of noise this pattern in the direction of the normal to the floor varied from a pressure maximum at floor level with successive maximum and minimum pressures as height from the floor increased. The amplitude of these maxima and minima damp out toward the ceiling to a level about 3 db down from that at the floor. Discrete tones produce a similar pattern with the minima, however, being very close to zero pressure and the maxima 6 db above the level that would exist at the point for the same source radiating into free space. The directivity of the source adds sufficient complexity to require a computer program. If we are concerned with the near field, we shall again require a computer program to use Eq. (8.23) to predict the character of the sound field. It is an assumption that Eq. (8.23) applies equally well for sound pressure fields where sound pressure levels are above

140 db re 0.0002 μbar. If we make this assumption, a computer program could include Eq. (8.23) and provide analytic predictions of the sound field in the Sonic Fatigue Facility. Experimental verification could be accomplished by sampling the sound field in the vertical direction at several locations in the chamber.

9. EXPERIMENTAL INVESTIGATION

The RTD siren operation will have the capabilities of producing discrete frequency or narrow band noise signals. An understanding of finite amplitude propagation for both is, therefore, desirable. In Sections 2-7 we have discussed the case of discrete frequency signals. In Section 8, broad band noise was treated analytically. In this section experiments with band limited noise signals are described.

9.1 REVIEW OF LITERATURE ON INTENSE BROAD BAND NOISE

That portion of the literature of finite amplitude sound concerned specifically with the propagation of high intensity acoustic noise signals is quite limited. In our search of the literature we found two papers by Ackerman[18,19]. The first is an attempt at a theoretical treatment while the second is a limited attempt at the experimental verification of the theory. The frequency band selected for the experimental work, however, was in the frequency range of 15 kHz to 50 kHz, well above the frequency range of interest for the RTD Facility. In addition, overall sound pressure levels were in the range of 110 to 135 db, while levels as high as 170 db are of interest here. Ackerman's theory predicts the effects of nonlinearity of the medium at high sound pressure levels to be the generation of sum and difference frequencies. Energy is thereby removed from the original frequency band and spread over larger parts of the spectrum. A quantitative description was developed for the case of 1/2 octave bands of plane wave acoustic noise three meters or less from the generator. At 15,000 Hz this distance, three meters, corresponds to 130 wavelengths.

The main siren bank at the RTD Facility produces acoustic energy of significant amount in the frequency range of approximately 150 to 2000 Hz. In this frequency range sound pressure levels as high as 165 db re 0.0002 μbar for a bandwidth

of 50 Hz have been measured in the near field of the sirens. For frequencies in the lower part of this range, 150 to 500 Hz and at levels below 170 db, essentially two regimes are possible, according to the theory. At sound pressure levels of up to 130 db, infinitesimal solutions are valid, that is, no significant finite amplitude effects are expected to occur. At sound pressure levels above 130 db "sum frequencies" build up but a shock wave does not form in three meters even at levels of up to 170 db. In the second frequency range, 500 Hz to 2000 Hz, the upper limit at which infinitesimal theory is still valid is lowered to about 110 to 120 db SPL. The lower level occurs at the higher frequency. At sound pressure levels between these levels and about 155 db "sum frequencies" build up although no shock wave is possible. Above this level the theory fails to offer a prediction.

The high frequency sirens can produce significant acoustic energy in the frequency range between 500 and 9600 Hz. It is, therefore, of interest to consider the nonlinear propagation of acoustic signals up to 9600 Hz as well. For frequencies above 2000 Hz, the same regimes as those from 500 Hz to 2000 Hz also occur. However, the sound pressure level regime for each successive frequency range is correspondingly lower. Thus, one is to expect the growth of "sum frequencies" at sound pressure levels as low as 105 db. The theory again fails at levels above 155 db at these frequencies. The theory adds one further prediction for noise bands at these higher frequencies. At sound pressure levels of 150 db shock formation cannot occur because of excessive attenuation of the "sum frequencies" generated by nonlinearities in the medium. It is to be noted that the theory offers no prediction at levels above 150 db in the upper end of this frequency range, about 500 Hz to 10,000 Hz.

The experimental results have been confined to the high sonic and low ultrasonic frequency range. In this range, the excessive absorption of the medium for the fundamental and

whatever "sum frequencies" are generated is the major factor. As a consequence, shock formation is precluded in the theory even at very high sound pressure levels up to 170 db. At the lower sonic frequencies of interest here, significant energy can be anticipated in the "sum frequencies" and the propagation of bands of noise at the higher sound pressure levels can be expected to be significantly different.

9.2 EXPERIMENTAL PROCEDURES

The nonlinearity of the basic equations applicable to sound propagation at these sound pressure levels implies that the simple summation procedures of the linear theory are not per se applicable. Thus, one cannot say a priori, that integration of pure tones over the band of interest constitutes a solution to the problem in the nonlinear case. It is for these reasons that we have undertaken an experimental investigation of the propagation of plane waves of acoustic noise.

The major experimental limitation was the generation of noise signals at the sound pressure levels of interest (up to 170 db) without initially introducing a significant level of harmonic distortion. This limitation required that the sound be generated with multiple transducers each operating at a low power level. The low power level per transducer required a large number of transducers whose sound energy output is converged to a narrow channel to raise the intensity to the degree required.

For this purpose use was made of the high intensity progressive sound tube facilities at the Riverbank Acoustical Laboratory in Geneva, Illinois. These facilities are described in Ref. 20 and briefly summarized in Appendix B. For this program the low frequency and medium frequency impedance tubes were used.

The low frequency tube used has a usable length of 20 ft (6.10 meters) and a diameter of 3 in. (7.5 cm). This was terminated

by a non-reflecting termination consisting of a wedge of acoustically absorbing material. The cut off frequency, f_c, the frequency of the first cross mode, for a cylindrical tube of radius, a, is given by Morse[21] as:

$$f_c = 0.586\ c/2a$$

For a 3 in. tube the cut off frequency is 2650 Hz. No difficulty was experienced in propagating bands of noise down the tube at levels up to 150 db SPL at frequencies as high as 1000 Hz.

The sound source for this tube is a bank of 49 speakers arranged in a square array of 7 by 7. The speakers were 8 in. cone loudspeakers, Jensen P8-PC. The arrangement of the speakers, their power handling capabilities, and efficiency are discussed in Ref. 20 together with construction and acoustical performance of the exponential horn coupling the speakers to the tube.

In order to attain higher levels at frequencies from 100 Hz to 2000 Hz we used the medium frequency tube. The details of this facility are also discussed in Ref. 20. The modification to this facility made for this experiment included: (a) adding a ρc termination, (b) adding a 3 ft section to the working length of the tube, and (c) replacing the power amplifier with the Savage 1 kilowatt audio amplifier. With 10 percent band limited noise having center frequencies 1500 Hz and 2000 Hz could be produced at sound pressure levels of 130 db re 0.0002 μbar.

In each tube the microphone can be moved down the axis of the tube with its diaphragm normal to this axis. Our procedure was to excite the drivers with a 10 percent band limited noise, position the microphone at a known distance from the cross section where the ρc ending began, and to record the microphone output on a Magnecorder, Model PT6BA magnetic tape recorder. A calibration signal of a pure sinusoid at a known

SPL and at the center frequency of the noise band was also recorded on the tape.

Simultaneously with the recording of the noise signal at a given station this station was identified on a second channel. These tapes were made into tape loops, one for each station at which analysis was to be performed. The loops were played through the Ampex recorder and the sound pressure level in a 10 Hz band relative to that of the calibrate signal was measured using the Quan-Tech Laboratories Model 303 wave analyzer. This was done in two ways. In the first, each harmonic of the fundamental on a given tape loop was measured using the meter reading of the wave analyzer directly. The peak level in the frequency region around the harmonic was sought and recorded.

In a second approach the tape recorder signal was presented to the Quan-Tech wave analyzer whose output was presented to a Bruel and Kjaer Type 2305 level recorder. The level recorder was driven synchronously by the Quan-Tech wave analyzer. Writing speed and paper speed on the level recorder were adjusted to provide maximum detail compatible with stability and reproducibility. A five second tape loop was completely analyzed over a frequency range of from 200 and 10,000 Hz in approximately one hour. When empty reels of tape were played through this system, the noise level in a 10 Hz band was at least 70 db down from the peak level of the fundamental at all frequencies above 250 Hz.

It is desirable to have a signal output from the drivers and the exponential horn as free as possible from harmonic distortion. To establish how well this requirement had been achieved we probed the sound field immediately in front of the speaker bank and for a distance of 42 in. into the horn from the plane of the speakers. A 10 percent bandwidth of noise with a center frequency of 250 Hz at a level of 157 db was generated.

Sound pressures were recorded as a function of distance from the plane of the speakers along the axis of the horn. For each of eight microphone positions, the recordings were made into tape loops and analyzed. The second and third harmonic distortion, that is, the difference in level between the first and second and between first and third harmonic components at each point expressed in db is plotted as a function of distance in Fig. 9.1. Distortion products follow a standing wave pattern similar to the standing wave of the fundamental (not shown).

We assume that strong reflections occur at the transition from the horn throat to the constant diameter experimental section. The cross-section is continuous in this transition region, but the rate of change of section is discontinuous. Consequently there is an impedance discontinuity giving rise to reflections and thereby standing waves. The variation in amplitude of the fundamental, as well as that of the second and third harmonic follow the typical standing wave pattern usually observed. The wavelength corresponds to the fundamental frequency with only second order perturbations at the harmonic frequency. Moreover the harmonic distortion appears to predominate at the pressure maxima. This leads to the supposition that the harmonics are mainly generated in the concentrator horn rather than in the transducers or amplifiers. A reduction of standing wave patterns in the coupling horn might be achieved by changes in the horn design and would lead to some slight reduction in the initial distortion in the measuring section. Such modifications were outside the scope of the present project and some initial distortion in the test section had to be accepted.

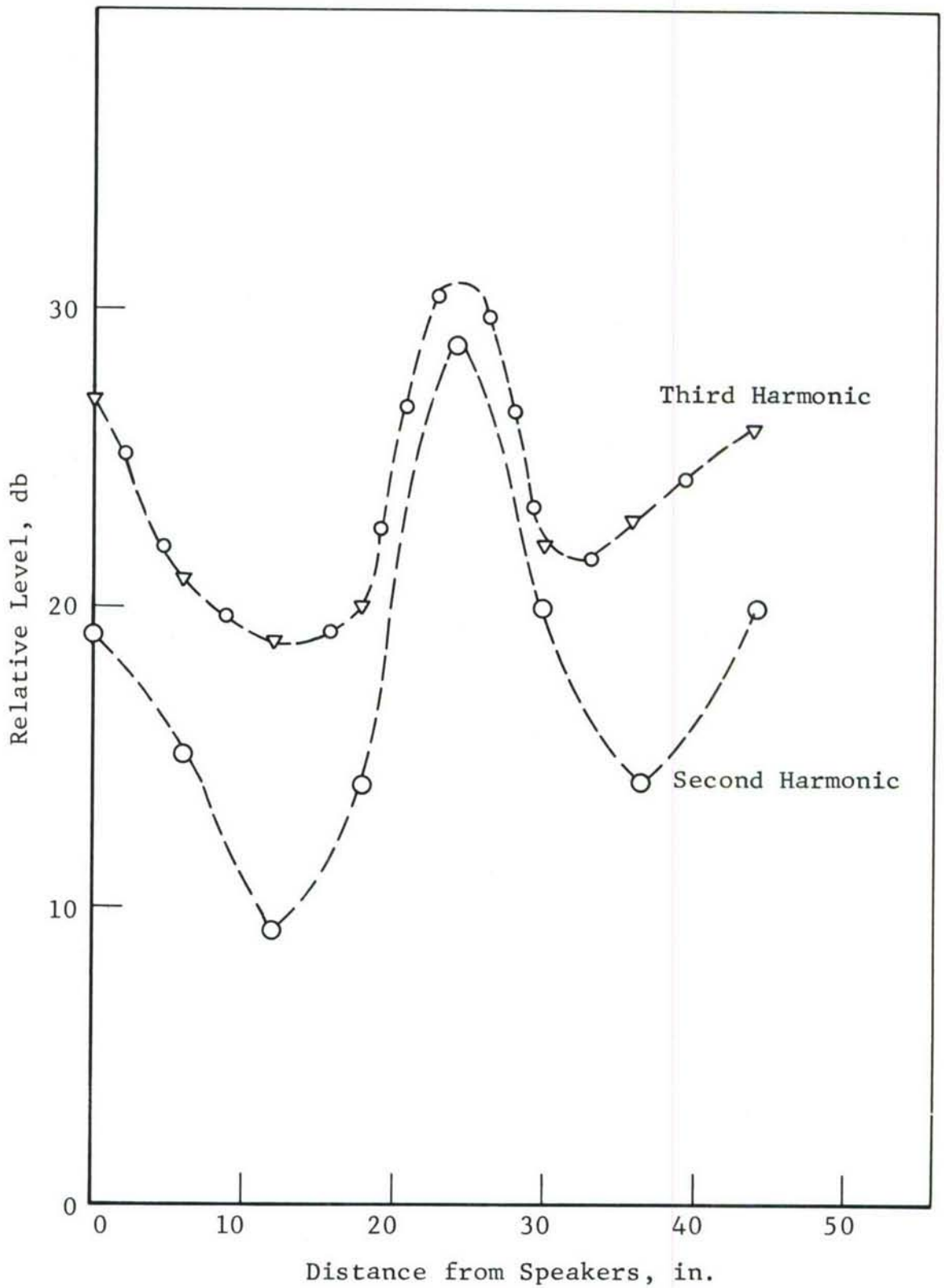

Fig. 9.1. Level of Second and Third Harmonic Components below the Level of the Fundamental as a Function of Distance from the Speakers in the Horn Coupling Section. (Band limited noise bandwidth 10 percent mean frequency 250 Hz at 157 db re 0.0002 μbar near speakers.)

The measurements made to establish the extent of harmonic distortion introduced by the speakers and by nonlinear propagation effects in the horn were not conclusive. However, harmonic distortion in the signal at the entrance to the acoustic tube was sufficiently low so that the growth of harmonics could be observed and measurements could be made.

Measurements of harmonic content of the signal in the tube entrance at the horn transition for a band of noise with central frequency at 800 Hz and overall SPL of 145 db showed the second harmonic down 30 db from the fundamental and the third harmonic down 50 db. Levels of fourth and higher harmonics were below the noise threshold of available instrumentation.

The lowest central frequency used for the narrow band (10 percent bandwidth) noise signals in the study was 300 Hz. Figures 9.2 and 9.3 relate to the measurements made at this frequency. Figure 9.2 presents spectral analysis of the recordings of the noise signal at a distance of 115 in. from the entrance to the tube. The overall noise level for Fig. 9.2 was 130 db. For a level of 110 db no distortion was measurable. In Fig. 9.3 we have presented the analysis at the entrance to the tube, at the distance of 115 in. and at a distance of 230 in. The overall sound pressure level was 160 db.

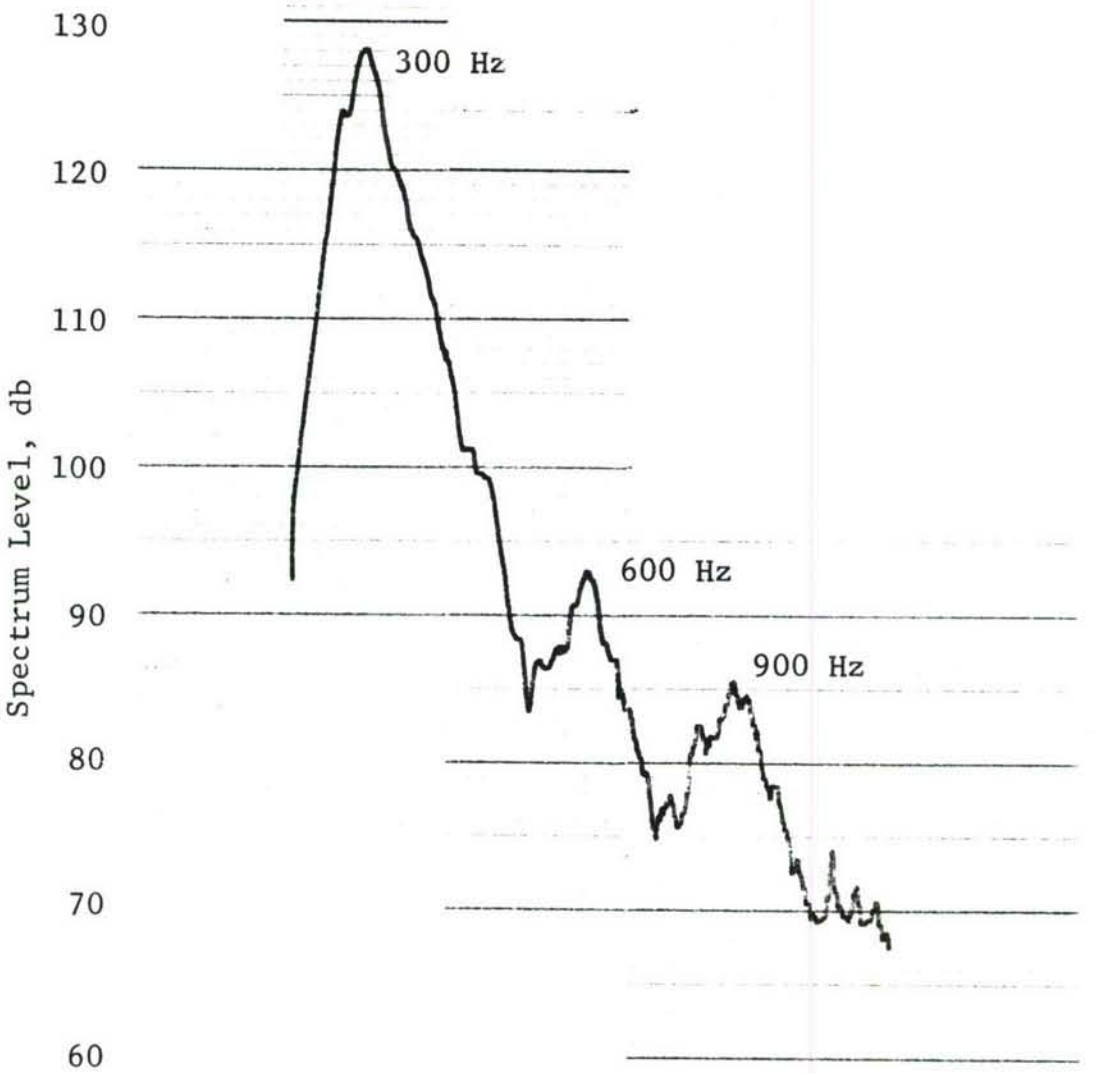

Fig. 9.2. Spectrum of Sound of a 10 percent Band of Noise Analyzed with a 10 Hz Bandwidth Analyzer. Microphone 115 in. from start of straight section of acoustic tube.

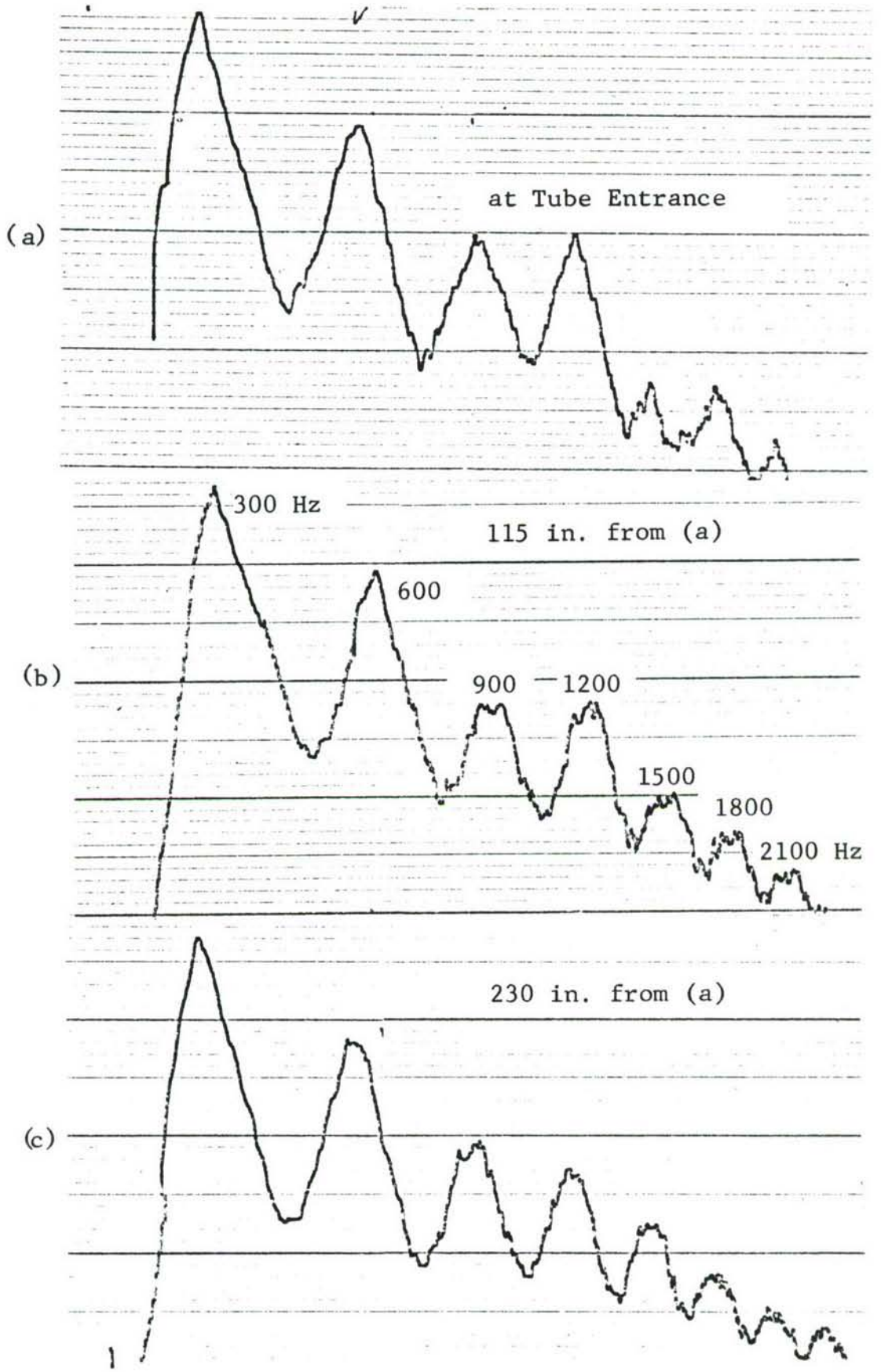

Fig. 9.3. Analysis of Growth of Distortion of 10 Percent Bandwidth Noise at 160 db Analyzed with 30 Hz Filter.

At the overall level of 130 db, Fig. 9.2 , energy is present in the second and third harmonic but their levels are 35 db and 42 db lower than the fundamental. At an overall level of 160 db (Fig. 9.3), however, there is measurable energy at even the seventh harmonic, while the lower harmonics, second and third, have levels within 8 db and 19 db respectively of the fundamental at a distance of 115 in. from the speakers. The high level of energy in the second and third harmonics at the position nearest the opening to the tube from the horn together with significant energy in the fourth and fifth harmonics is not understood. Such results were not observed at higher frequencies at the very highest overall levels. The investigation of the sound field in the exponential horn at comparable overall levels, 157 db, and at a frequency of 250 Hz did not suggest this result. Even this degree of harmonic content, however, represents only a small distortion of the noise signal. It cannot be said, for example, that a shock wave is present.

In Fig. 9.4 we have plotted the variation of sound pressure level in all harmonics present versus distance down the tube from the entrance. The central frequency is 300 Hz and the overall level is 160 db. At this frequency the working length of the tube was about 1.6 wavelengths. There appears to be no significant change in level with distance for this distance in the first four harmonics. The fifth and sixth harmonics have increased in level about 2 to 3 db over 1.6 wavelengths.

The appearance and growth to a maximum level of harmonics in a noise signal is well illustrated in Fig. 9.5. Here the central frequency was 800 Hz and the overall level for the signal was 145 db. This was the maximum level attainable in the tube at this frequency. The wavelength of sound at 800 Hz is 0.43 meters so that the working lengths of the tube correspond to 13.7 wavelengths. The appearance of successively higher harmonics and their rapid growth to peak levels as the wave progresses down the tube is a prominent feature. The levels of

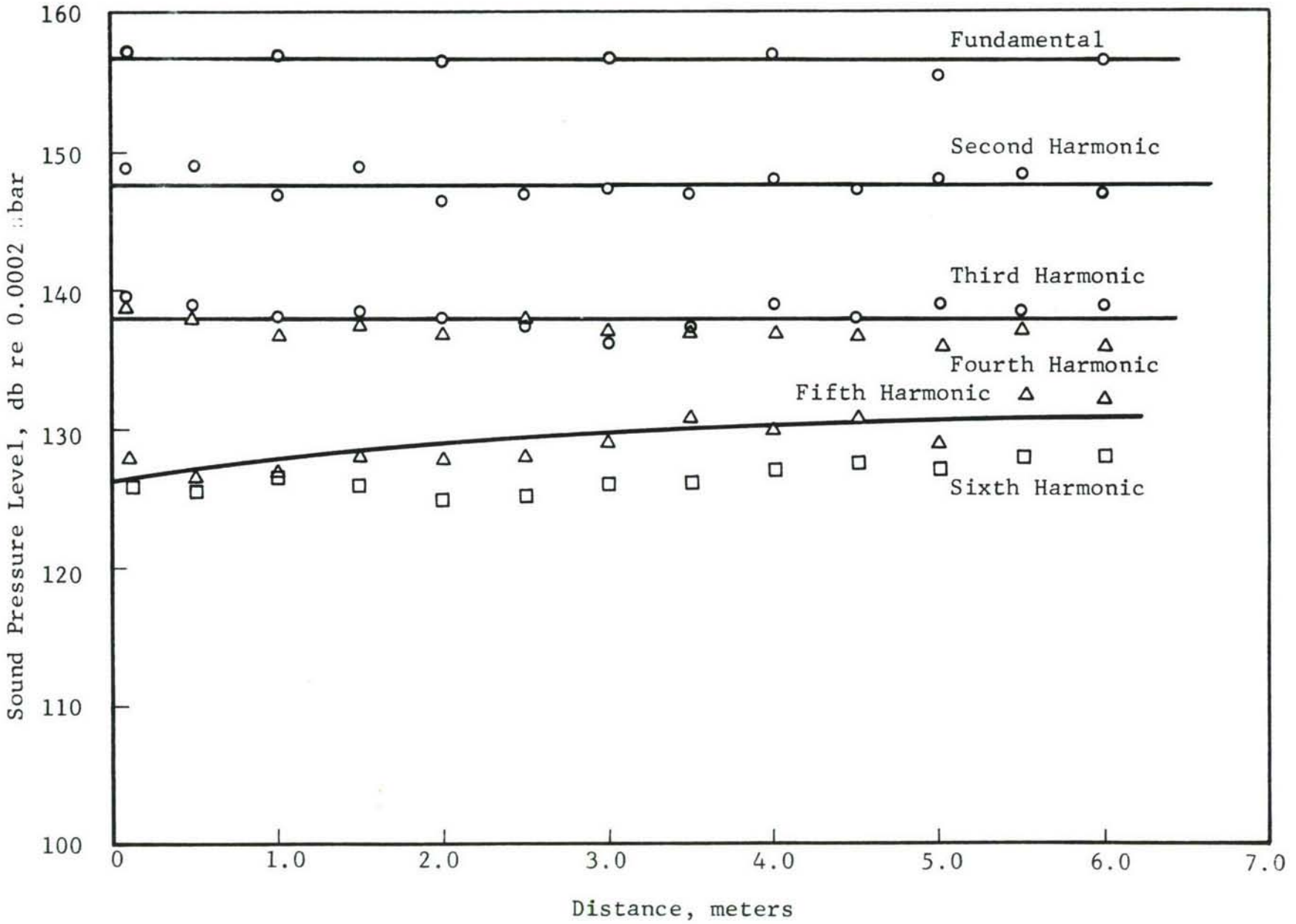

Fig. 9.4. Growth of Harmonics of a Plane Wave of Narrow Band Noise in an Impedance Tube (Overall sound pressure level in 10 percent bandwidth 160 db, central frequency 300 Hz).

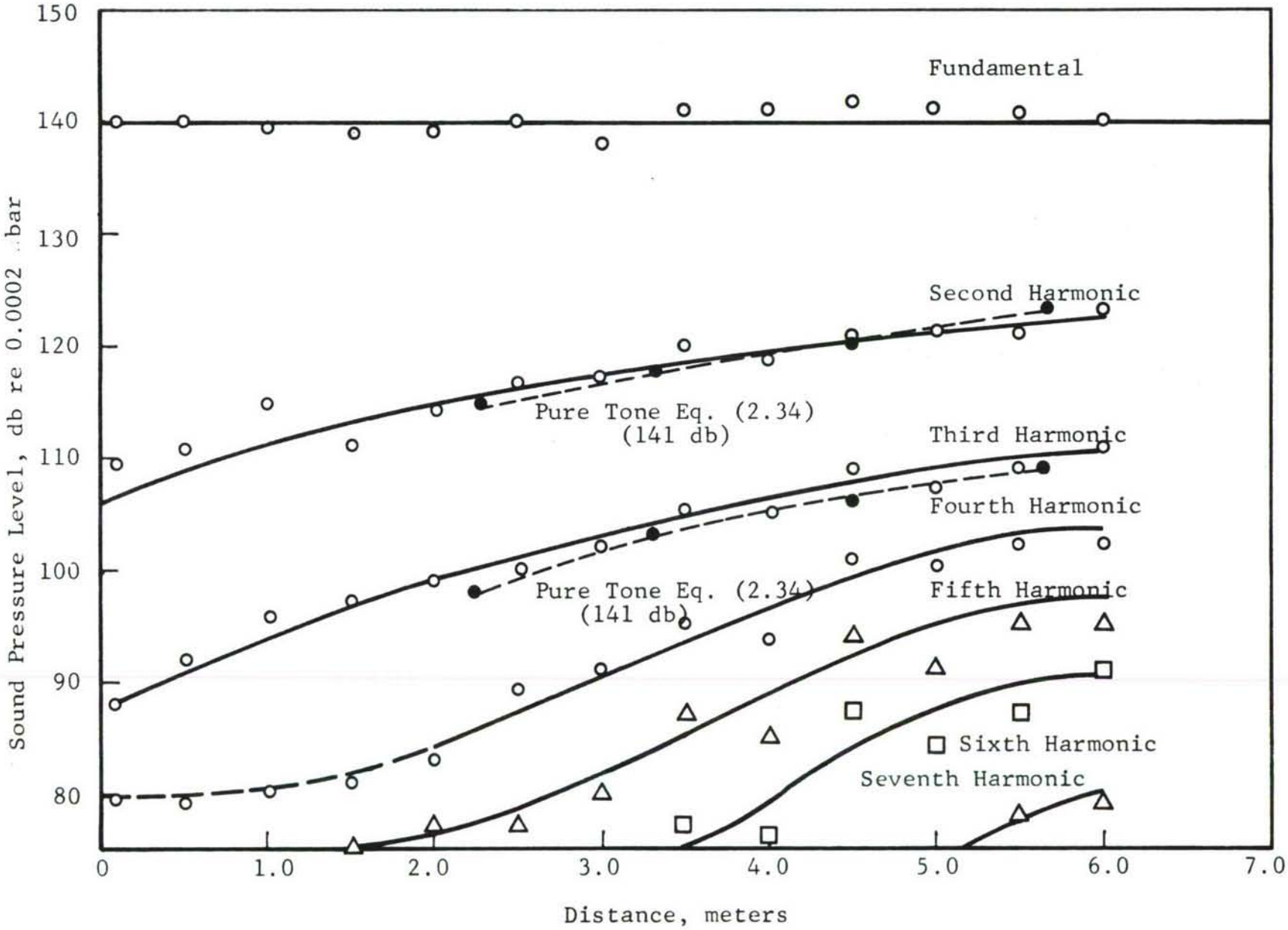

Fig. 9.5. Growth of Harmonics of a Plane Wave of Narrow Band Noise in an Impedance Tube (Overall sound pressure level in 10 percent bandwidth 145 db, central frequency 800 Hz).

the second and third harmonics at the entrance to the tube from the exponential horn are 30 db and 50 db down from the fundamental. Therefore, the possible distortion produced in the signal by the speakers and the horn do not obscure the effects of nonlinear propagation in the tube. At overall levels of this order the levels attained by harmonics higher than the third will not be significant for operation of the Sonic Fatigue Facility. Within the tube these higher harmonics rise rapidly initially but over the distance of four to five wavelengths have already passed their peak. The maximum level attained for the second harmonic was 16 db below the fundamental and for the third harmonic was 30 db below the fundamental.

The uniformity of the sound pressure level of the fundamental along the length of the tube attests to the quality of the termination. The standing wave ratio seems to have been below 3 db. The quarter wavelength peak to valley distance is approximately 0.1m for 800 Hz, hence the apparent irregularity of the point shown in Fig. 9.5, some of which come close to maxima and some are near minima of the small residual standing wave pattern. This residual standing wave pattern tends to obscure the growth of harmonics near the far end of the tube. Indications are strong that the rate of growth of the harmonics decreases in the manner indicated for pure tones in Fig. 2.3. Comparison with pure tone assumptions is shown dotted in Fig. 9.5 and discussed together with a similar curve at 1000 Hz in Section 9.3.

In plane wave propagation the power of harmonics is less than 2 percent of the total after travelling a distance of fourteen wavelengths at an initial fundamental sound pressure level of 145 db at 800 Hz. This two percent reduction in fundamental level is not discernible among the residual standing wave fluctuations.

These results pertain to a signal confined to the interior of a tube. They, therefore, represent upper bounds for

the case of the sirens of the Sonic Fatigue Facility where spherical spreading will decrease intensity within the wave as it propagates out into the room. With spherical spreading propagations of the wave for a distance of 6 meters would decrease the sound pressure level in the signal 14 db below its level at 1 meter from the source. This applies to all harmonics as well. It is directional, nevertheless, spreading of the wave energy must occur and the transfer of energy into the higher harmonics must be less efficient than is true for the acoustic tube.

Figure 9.6 presents comparable results for a band of noise 10 percent bandwidth and centered at 1000 Hz. Again the second harmonic has reached a peak at a level 16 db below the fundamental and the third harmonic has reached a peak at a level 26 db below the fundamental.

At sound pressure levels of 130 db re 0.0002 μbar or lower for frequencies below 500 Hz and at 110 db or lower for the frequencies of 800 Hz and 1000 Hz, there was no evidence of a growth of harmonic content as the noise signal propagated down the tube. For these frequencies and at these levels the infinitesimal theory clearly holds. Although a small harmonic content is present in the signal at the entrance to the tube, it does not increase at any harmonic. These results are in agreement for these frequencies with Ackerman's theory. We have presented a resume of the data for these cases in Table 9.1. Data for three stations are included (a) near the termination, (b) near the half way point in the tube, and (c) at the speaker end of the tube.

At the maximum levels achieved in the tube and the path length of travel for the signal, no shock wave could be said to have formed. This is true even for the case of the signal with central frequency of 300 Hz and overall sound pressure level of 160 db. There was a significant transfer of energy into the second and third harmonics at the higher overall sound pressure levels above 145 db which could be attributed to

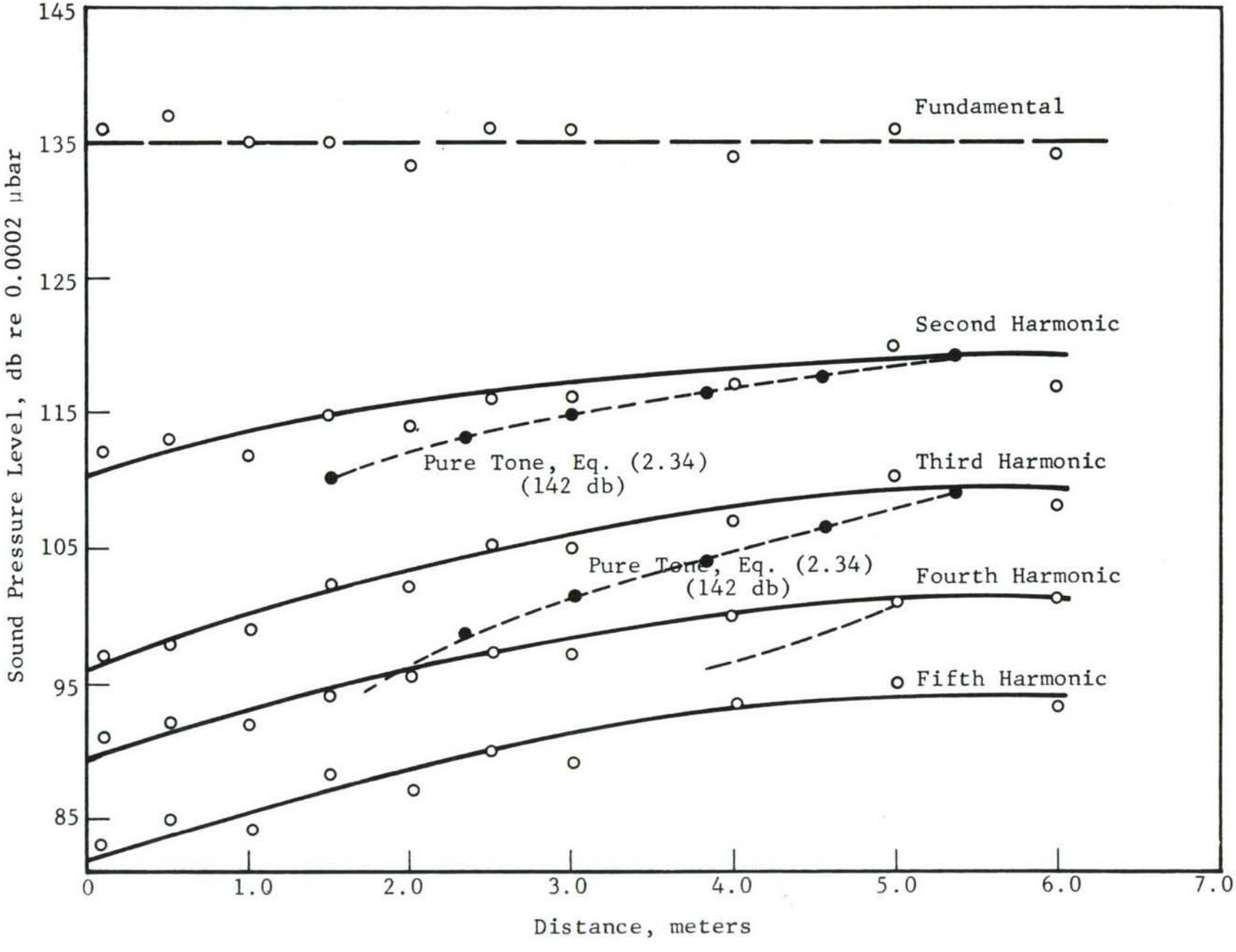

Fig. 9.6. Growth of Harmonics of a Plane Wave of Narrow Band Noise in an Impedance Tube (Overall sound pressure level in 10 percent bandwidth 145 db, central frequency 1,000 Hz).

nonlinear effects in propagation of the signal through the tube. The maximum transfer of energy into these harmonics, however, brought them to levels no higher than 2 percent for the second harmonic and 0.1 percent for the third harmonic of the energy in the fundamental. For the higher harmonics the energy content at the most is negligible. The harmonic distortion in the sound output of the sirens will be expected to be much more significant than the additional transfer of energy into the higher harmonics attributable to nonlinear propagation in the volume of the room.

TABLE 9.1

LIMITED GROWTH OF HARMONICS IN 10 PERCENT BAND LIMITED NOISE FOR RELATIVELY LOW SOUND PRESSURE LEVELS

Frequency (Hz)	SPL db re 0.0002μbar	Distance from Start of Straight Section (inch)	db Below Fundamental				
			$F-H_2$	$F-H_3$	$F-H_4$	$F-H_5$	$F-H_6$
300	110	0	32	37	39	41	43
		120	30	34	36	38	39
		236	28	31	35	37	38
300	130	0	37	44	54	58	65
		120	36	43	54	58	63
		236	37	45	54	58	61
500	110	0	34	45	49		
		120	34	43	50		
		236	36	44	50		
500	130	0	32	47	60		
		120	32.5	47.5	58.5		
		236	29	47	58		
800	110	0	35.5	46.5			
		120	37	49			
		236	37	51			
1000	100	0	43	46	52		
		120	44	48	54		
		236	44	48	53		

9.3 COMPARISON OF EXPERIMENTAL RESULTS WITH COMPUTATIONS

It was pointed out in Section 2.6 that distortion effects may be expected in band limited noise in the same way as in pure tones, but the distortion may bear a different relationship to the root mean square amplitude because of differences in the distribution of peak amplitudes. In Fig. 9.5 the growth of the second and third harmonic of a pure tone of the same RMS amplitude is indicated and seen to be very close to the amplitude of the distortion products measured for the noise. Such agreement might be fortuitous. In Fig. 9.6 the growth of harmonics of a pure tone 7 db higher in intensity than the noise is shown. The measured rate of growth is seen to be less than that computed for the tone. If a lower level tone had been chosen for comparison a lower growth rate, but also a lower level of distortion products would have been obtained. It is possible that the discrepancy may be accounted for in part by the finite initial distortion.

Further theoretical and experimental investigations along this line would seem appropriate.

10. ROOM TREATMENT

It was concluded in Sections 2-9 that effects in the room at points remote from the siren are relatively small compared with nonlinear effects in the siren horns.

The interactions due to reflections at the floor for the semi-anechoic mode of operation and due to the reflections at walls and floor in the semi-reverberant mode may be computed from the treatment in Section 7. For normal incidence where long wave trains are superimposed over considerable distances slight additional distortion and intermodulation is predicted. However, the shape of the room and the absence of a wall parallel to the plane of the sirens limits normal incidence to an insignificant portion of the total sound energy. For oblique incidence the interaction will be only over a limited region, where incident and reflected sound waves overlap. Moreover, positive and negative pressure regions overlap alternately so that the overall effect tends to cancel out. This means that the nonlinear effects are simply those of direct propagation from an effective image source. The contribution of reflected waves to nonlinear distortion and intermodulation is negligible for practical purposes; because, as previously stated, nonlinear propagation effects in the spherical propagation region are small in the frequency and intensity regions under consideration, and also because the first reflections are all near grazing incidence.

Thus, room conditions whether reverberant or anechoic do not change any of the basic contributions of nonlinear effects.

11. RECOMMENDATIONS

11.1 FACILITY USE

The harmonic content of the sound should be taken into account when setting up specific sound spectra in the room. Direct generation of high frequency components may be reduced due to the generation of these components by distortion in the lower frequency component generators.

11.2 MEASUREMENTS AND TESTS

The mathematical treatment predicts the level of the harmonic components for finite amplitude generators. However, at the highest amplitudes the extrapolation is somewhat uncertain and direct measurements are recommended. Some of these measurements have already been undertaken. It is recommended that these measurements be extended to a more detailed mapping of the sound pattern of a single siren. The amplitude of both fundamental and of each harmonic should be measured at a convenient distance from the source as a function of the angle between the microphone direction and the horn axis. Two planes should be chosen, preferably the horizontal plane and the plane containing the diagonal of the square horn mouth. If the directional characteristics of the sirens is found to be very different in these two planes so that interpolation is uncertain, intermediate planes inclined at 22.5°, 11.25°, and 37.75° should be chosen to augment the data.

These data will be needed if precise fields are to be computed in the facility. The directional characteristics of the sirens may be amenable to computation. In that case a more limited experimental program can be set up in which these characteristics are measured at a very limited number of frequencies to check the computations.

11.3 FACILITY MODIFICATIONS

11.3.1 Low Frequency Horns

Facility modifications have been contemplated to extend the capability to lower frequencies by modifying some of the horns to have a lower cut off frequency. This modification should be limited to the minimum number of horns to be used at low frequency. At small amplitudes the cut off frequency has negligible effect on high frequency performance. At large amplitudes the distortion is greater if the sound is maintained at the high intensity for a long time in a longer horn.

11.3.2 High Frequency Horns

Some consideration may also be given to the relative merits of reducing the high frequency distortion by increasing the flare in some of the horns. The cut off frequency will thereby be increased, thus adversely affecting the flexibility of the facility. A compromise must be established taking into account the expected use of the facility. In other words, if the distortion is considered unimportant, and a need for high intensity at low frequency is foreseen, a larger number of low frequency units would be desirable, than if maximum output with low distortion is required at high frequencies.

11.4 FURTHER THEORETICAL ANALYSIS

The importance of the distortion produced in the horn of the siren (Section 3) was not realized sufficiently early in the program to devote the time necessary to extend existing theories to the very large amplitudes involved. Existing theories were cautiously extrapolated, but the precise computation of the value of the distortion products requires a more sophisticated theory. The theory used is essentially a second

order approximation and is valid for moderate distortion levels. The theory needs to be taken to a higher order of approximation to establish the precise level of distortion products. This knowledge would permit a more exact evaluation of the relative merits of using horns specifically designed for narrow frequency regions as discussed under 11.3.

11.5 EXPERIMENTAL STUDIES

11.5.1 Distortion in Siren Horns

The portions of the curves shown dotted in Fig. 3.1 may also be verified or modified by an experimental study. A simple series of tests would consist of placing a suitable transducer close to the mouth of a siren and measuring the amplitude of each of the harmonics generated (including the fundamental) as a function of power input to the siren. The experiment would be repeated for different frequencies over the full range of the siren capability. A study of this kind is relatively easy to undertake and is strongly recommended to augment or replace the theoretical study of Section 11.2.

In addition it would be useful if the directional patterns of the radiation of the sound from the sirens be determined experimentally. This will be needed if the sound field in the facility is to be computed. The question of the radiation of a sound of a certain frequency may be affected by the presence of other sounds. Thus the radiation of a 3 kHz component when generated as a fundamental may be different from the radiation pattern of the sound of this frequency when it is the second harmonic of 1.5 kHz or the third harmonic of 1 kHz.

11.5.2 Other Nonlinear Effects

An experimental investigation of other effects studied in this report may also be of interest. This includes the reflection of simple large amplitude sounds and the interaction

of sounds of different frequency generating intermodulation products at the sum and difference frequencies. The study of the precise level of distortion in horns (Section 11.5.1) should be given high priority.

11.5.3 Noise

The magnitude of the nonlinear effects on initially simple harmonic pressure fluctuations is not readily translated to random signals; Sections 2.5, 8, and 9.3 indicate some of the difficulties involved. It is suggested that an experimental program be set up in the high intensity facility in which amplitudes of the fundamental and the first few harmonics be measured at various distances on the axis of a siren at different levels of pure tones and narrow band noise. Simultaneous theoretical development as in Section 8 would also be appropriate.

12. CONCLUSIONS

The nonlinearities introduced by the medium for finite amplitude sound waves introduce harmonics into the sound waves generated by the sirens. This means that in order to generate a predetermined spectrum in the facility allowance must be made for this effect. The effect can be reduced by redesigning some of the horns to have higher cut off frequencies. In any case if lower cut off frequency horns are to be used on some of the sirens in order to generate lower frequency sounds, the changeover should be limited to the number needed for the low frequency generation. The use of a horn with a low cut off frequency for high frequency generation will increase the distortion produced.

Because of the large unavoidable distortion in the siren horns, the much smaller additional effects in the room may be neglected.

REFERENCES

1. Blackstock, D.T., "Thermoviscous Attenuation of Plane Periodic Finite Amplitude Sound Waves," J. Acoust. Soc. Am., Vol. 36, p. 534, 1964.

2. Cook, B.D., "New Procedure for Computing Finite Amplitude Distortion," J. Acoust. Soc. Am., Vol. 34, p. 946, 1962.

3. Fubini-Ghiron, E., "Anomalous Propagation of Sound Waves of Finite Amplitude" (in Italian), Alta. Freq., Vol. 4, p. 530, 1935.

4. Keck, W. and Beyer, R.T., "Frequency Spectrum of Finite Amplitude Ultrasonic Waves in Liquids," Third International Congress on Acoustics, Stuttgart, Germany, 1957. Phys. Fluids, Vol. 3, p. 346, 1960.

5. Hargrove, L.E., "Fourier Series for the Finite Amplitude Sound Waveform in a Dissipationless Medium," J. Acoust. Soc. Am., Vol. 32, p. 511, 1960 (L).

6. Olson, H.F., Acoustical Engineering, D. Van Nostrand Co., Inc., Princeton, N.J. (1957), p. 225.

7. Thuras, A.L., Jenkins, R.T. and O'Neil, H.T., "Extraneous Frequencies Generated in Air Carrying Intense Sound Waves," J. Acoust. Soc. Am., Vol. 7, p. 173, 1935.

8. Laird, D.T. and Ackerman, E., "Spherical Waves of Finite Amplitude," WADC TR 5-463, July 1957.

9. Lin, C.C., "On a Perturbation Theory Based on the Method of Characteristics," J. Math. Phys., Vol. 33, p. 117, 1954.

10. Naugol'nykh, K.A., Solayan, S.I. and Klokhlov, R.V., "Spherical Waves of Finite Amplitude in a Viscous Thermally Conducting Medium," Soviet Physics--Acoustics, Vol. 9, p. 42, 1963.

11. Hunt, F.V., "Propagation of Sound in Fluids" (Chapter 3C), American Institute of Physics Handbook, McGraw-Hill Book Publishing Company, N.Y. (1957).

12. Sperry, W.C., "Perturbation Solutions for Nonlinear Plane Wave Equations of Acoustics," AMRL-TDR-63-62 (1963) and AMRL-TDR-63-63 (1963).

13. Raelson, V.J., "Solution for Nonlinear Plane Wave Equations of Acoustics by the Method of Functional Interrelationship of Dependent Variables," AMRL-TDR-63-63 (1963).

REFERENCES (Cont'd)

14. Blackstock, D.T., "Approximate Equations Governing Finite Amplitude Sound in Thermoviscous Fluids," GD-1463-53.

15. Petrovsky, I.G., Lectures in Partial Differential Equations (Chapter 4), Interscience Publishers (1954).

16. Abramowitz, M. and Stegum, I., Handbook of Mathematical Functions, National Bureau of Standards, Series 55 (1964), pp. 376-377.

17. Tyzzer, F.G. and Pernet, D.F., "Analytical and Experimental Investigation of the Acoustic Environment of the RTD Sonic Fatigue Main Test Chamber," FDL-TDR 64-26.

18. Ackerman, E. and Burnett, W.A., "Propagation Distortion of Bands of Acoustic Noise--I," WADD TR-60-232, 1959.

19. Oda Frijio and Ackerman, E., "Propagation Distortion of Bands of Large Amplitude Acoustic Noise--II," WADD TR-60-233, 1960.

20. Tyzzer, F.G., "Development of a Suitable Treatment for the ASD Sonic Fatigue Facility," ASD TDR-62-985 (1963).

21. Morse, P.M., Vibration and Sound, McGraw-Hill Book Publishing Company, N.Y. (Second Edition), (1948).

22. Robson, J., An Introduction to Random Vibrations, Elsevier Publishing Co. (1964), p. 50.

23. Naugol'nykh, K.A., "Propagation of Spherical Waves of Finite Amplitude in a Viscous Heat Conducting Medium," Soviet Physics--Acoustics, Vol. 5, p. 79, 1959.

24. Goldberg, Z.A., "Propagation of Plane Acoustic Waves of Finite Amplitude in a Viscous Heat Conducting Medium," Soviet Physics--Acoustics, Vol. 5, p. 117, 1959.

APPENDIX A

MEASUREMENTS OF SOUND FIELDS IN THE AFFDL FACILITY

Sound pressure levels were measured in the Facility with siren #2 only, siren #4 only, and both siren #2 and siren #4 operating together. Waveforms were observed for operating frequencies of 300 Hz and 1000 Hz. At 300 Hz distortion was reported to be low and detailed measurements were not further reported.

For a frequency of 1000 Hz waveforms of the sound were recorded immediately in front of siren #2 and at several locations in the room. The locations were chosen in a single plane normal to the plane of the sirens midway between #2 and #4 at distances of 6 ft. 2 in., 12 ft. 8.5 in., and 15 ft. 4 in. and heights of 3 ft. 11 in., 10 ft., 12 ft., 14 ft., and 16 ft. above the floor.

Spectrum analysis yielded a rather complex picture of the distortion at various points. This is attributed to the fact that the radiation pattern of the sirens is rather complex and the angle of the siren axis and the vector from the mouth of the siren to the measuring location changes with the measuring location, so that peaks or valleys of the radiation pattern may be close to different measuring points for the different harmonics.

The sound pressure level in front of siren #2 was 168 db and the 2nd, 3rd, and 4th harmonic were 10 db, 14 db, and 15 db respectively below the fundamental.

The largest distortion in the room was measured at the 12 ft. height above the floor at the 12 ft. 8.5 in. distance where the fundamental was 150 db and the 2nd, 3rd, and 4th harmonic were only 5 db, 10 db, and 11 db respectively below the fundamental; at most other locations the distortion was no greater

than immediately in front of the horn. It seems reasonable to explain this behavior by assuming that the harmonics showed side lobes in their radiation pattern in this direction.

The recorded waveforms are shown in Fig. A-1. Very distinct triangular shock waves are readily discerned. Some of the records have been inverted because no attention had been given to the phase of the microphone connection and the presentation of the shock with uniform polarity helps distinguish this feature in the record. The columns of oscillograms show simultaneous records of six microphones at a distance from the siren bank shown at the top of the column. The height of the microphone above the floor is shown in the left margin. The fourth oscillogram is the record of a monitor microphone located in the mouth of siren #2 for all conditions.

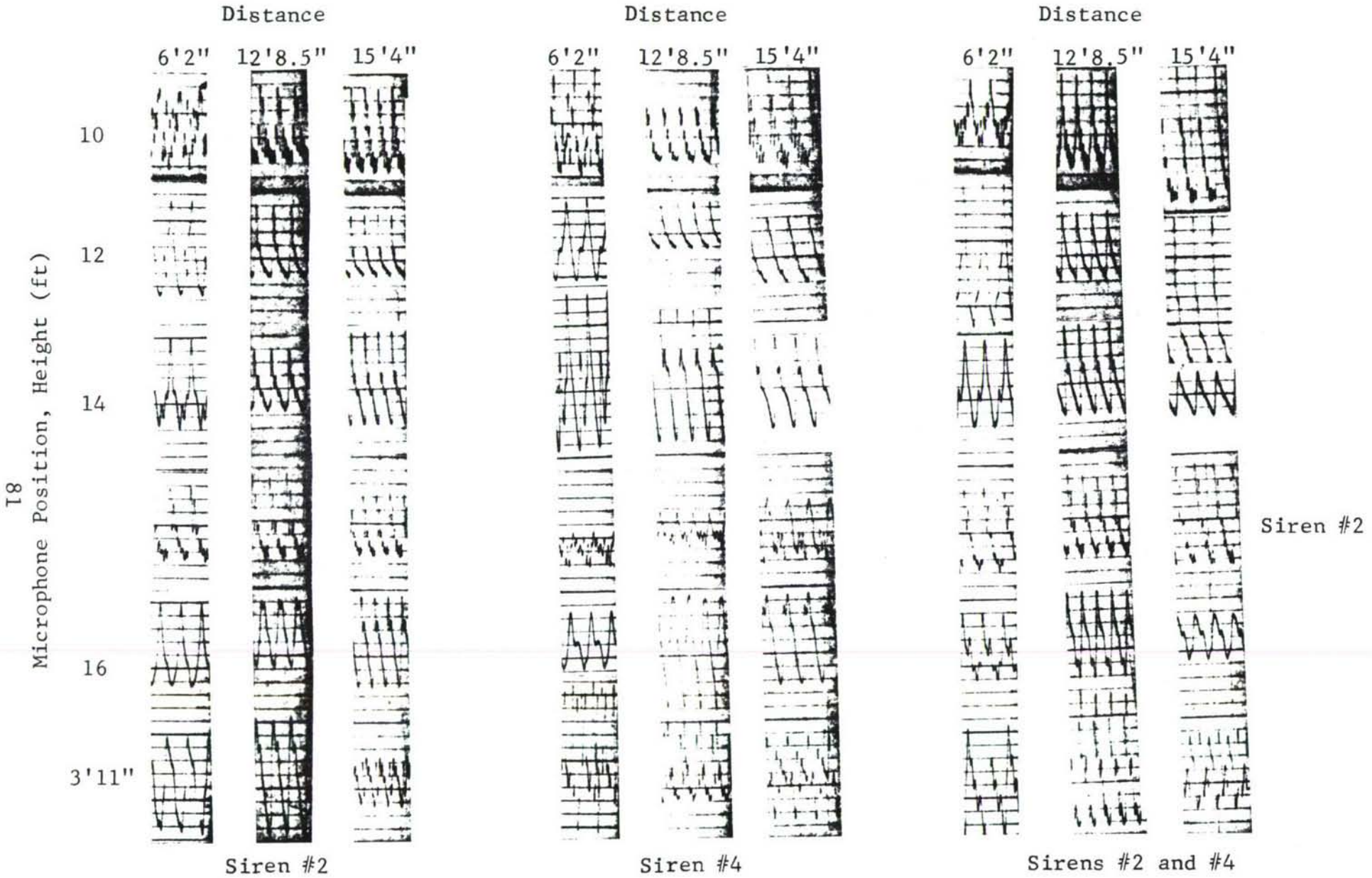

Fig. A-1. Sound Pressure-Time Function at 1 kHz at Wright-Patterson Air Force Base Sound Facility in Anechoic Mode.

APPENDIX B

HIGH INTENSITY TEST FACILITY AT RIVERBANK ACOUSTICAL LABORATORIES

Of the three high intensity acoustic tubes[20] available at the Riverbank Acoustical Laboratories, only the low frequency tube had adequate length to show appreciable nonlinear propagation effects. Though originally designed for the 20 to 300 Hz region, operation to 2000 Hz was quite successful.

A drawing of the low frequency impedance tube is shown in Fig. B-1. This tube was mounted in the center of a plywood box filled with sand approximately 8.5 by 12 in. in cross section in order to damp resonant vibrations of the tube walls. The horn sections coupling the low frequency tube to the drivers was also damped by sand. The minimum thickness of sand at all surfaces of the tubes and horn was 4 in. and over 6000 lbs. of sand were used.

The length of the low frequency impedance tube was set by the space available for the tube and its associated horn. The tube was 20 ft. long, the horn with its coupling section was 16.5 ft. long, and the sample holder was 6 ft. 4 in. long, giving an overall length of about 43 ft. In the 20 ft. tube length two minima in the standing wave pattern could be measured for frequencies above about 57 cps for any sample impedance. Below this frequency, measurements were in some cases restricted to one minimum point and one maximum with some loss in accuracy involved in calculation of the wave length and estimating the attenuation along the tube. The latter source of error was not very significant since the attenuation along the tube was small for the samples of high absorption which were measured.

The sound field inside the impedance tube was explored by a microphone mounted inside the impedance tube at the end of a probe tube. A tube was used instead of a rod in order to provide

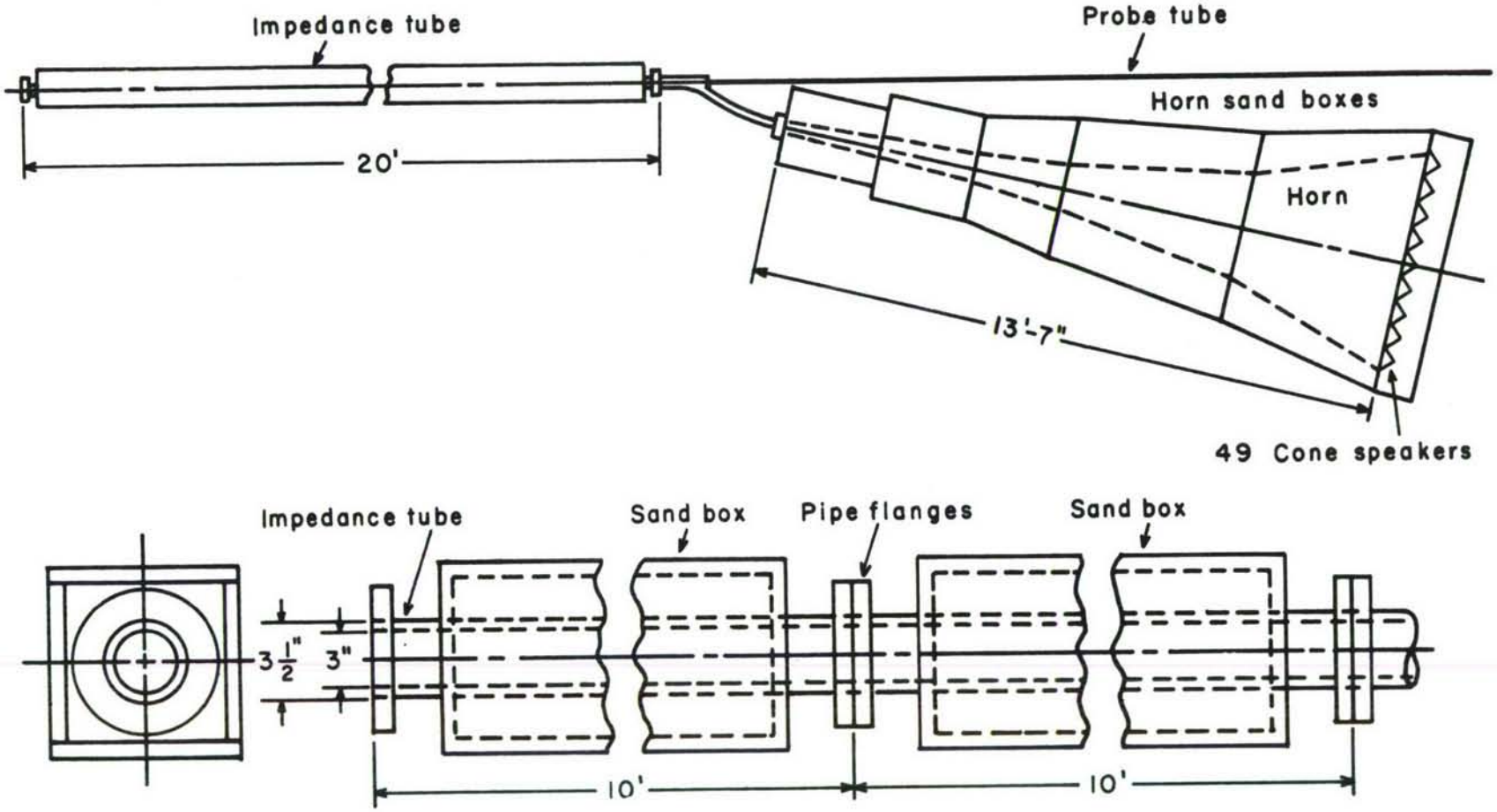

Fig. B-1. Low Frequency Impedance Tube.

a shielded conduit for the microphone cable. The probe tube passed through a felt lined bushing at the sound-source end of the impedance tube. The microphone end of the probe tube was supported by a three legged carriage with felt at the contacts between the carriage and the inside surface of the impedance tube. The felt at the microphone carriage supports and at the bushing provided vibration isolation for the microphone which is essential for accurate measurements of sound pressure. The microphones were supported by their electrical connections (thin wires) to the calibrate resistances and to the signal and calibration cables which were inside the probe tubes. The other end of the probe tube was clamped to a movable carriage which supported the microphone preamplifier.

The probe tube was 0.75 in. in diameter and about 23 ft. long. The preamplifier carriage was moved along a 2 by 5 in. aluminum channel by means of an endless chain driven by a sprocket. A steel tape loop attached to the carriage was used to determine the microphone positions.

The drivers for the low frequency tube consisted of 49 8 in. cone loudspeakers, Jensen P8-PC. The drivers were connected in a seven by seven array and each line of seven drivers in series was fused. It was found that the resonant frequency of all the speakers was not the same and, for frequencies near 50 cps, high intensities could not be attained without damage to the cone supports. Under this condition, a few speakers which were driven near resonance had excessive amplitudes and the others, off resonance, had much smaller amplitudes. A level of 140 db, however, could be obtained even in this resonance range.

The speakers were rated at 15 watts for broadcast program material. Using a "rule of thumb" conversion factor of one-half for continuous sinusoidal signal would give a rating of 7.5 watts per speaker. For the nominal impedance of 8 ohms, the maximum current rating is 0.96 amp. For the 7 by 7 array

the maximum input current is then about 7 amps and the maximum input power is 370 watts. Operation at 6 amps corresponding to 290 watts resulted in a voice coil temperature which caused discoloration of the voice coil forms, but few failures occurred except as noted for operation near resonance.

A pressure level of 160 db corresponds to an intensity of about one watt/cm^2 assuming that the impedance tube is terminated by ρc. The 3 in. diameter tube had an area of 45.6 cm^2 which gives an acoustic power requirement of about 45 watts. The efficiency of the driver and horn system (electrical input power divided by acoustic power in the impedance tube) was thus about 45/290 or 16 percent over most of the frequency range.

The speakers were mounted in a 71 by 69 in. plywood panel one inch thick and were spaced 8.5 in. on center. The panel was attached to the large end of the exponential horn which was coupled to the low frequency tube. The horn construction is described below. The space behind the speakers was a cavity of rectangular cross section, 68 by 66 by 8 in. This space was ventilated by means of a small blower. Lined ducts at the inlet and outlet openings for the cooling air were used to reduce the sound from the back of the speakers.

The cone loudspeakers were coupled to the low frequency impedance tube by an inverted exponential horn designed to provide an approximation to ρc loading for the loudspeakers. For design purposes the layer system was assumed to have high absorption and thus the impedance tube was terminated by a specific impedance of about ρc and the specific impedance looking into the source end was also approximately the same. The horn is considered as a transformer which matches the acoustical impedance of the small area at the impedance tube to the large area at the loudspeakers. The acoustical impedance is defined as the specific impedance divided by the area. Thus, a well designed

horn will transform the acoustical impedance at the throat $\rho c/S_1$ to $\rho c/S_2$ at the large end and give a desirable loading for sound sources at this end.

The horn was designed on the basis of the following specifications, a 3 in. diameter at the throat, a 59 by 59 in. area at the large end for mounting 49 8 in. loudspeakers, a cut-off frequency below 50 cps, and available space and cost requirements. The equation for an exponential horn of axial length d is

$$\exp(qd) = S_2/S_1$$

The flare constant q determines the cut-off frequency f_1 which is defined as

$$f_1 = qc/4\pi$$

For d equal to 13.6 ft. and S_2/S_1 equal to $(59/3)^2$ or 388, q is 0.44 ft^{-1} giving a cut-off frequency of 40 cps.

In building the horn it was decided, because of cost, to use flat plywood one inch thick for the greater part of the sides with some deviation from an exponential expansion in area. The length was divided into seven segments. The first was 19 in. long and was made of 1/4 in. sheet steel which was formed to have a circular cross section 3 in. in diameter at the impedance tube end and a square cross section at the other end. The following segments were made of plywood and were each two feet long. They were hollow pyramids with a square cross section. At each junction between segments, the width of the segment was fitted to the exponential curve specified in the preceding paragraph. The large end of the horn was closed by a 59 by 59 in. flat plywood panel on which the 49 loudspeakers were mounted in a seven by seven array approximately 8.5 in. on center.

The axis of the horn was inclined from the impedance tube axis as shown in Fig. B-1. The angle between the axes was about

14°. A flanged steel tube, 3 in. I.D. and about 3 ft. long was bent to connect the impedance tube and horn so that there was no interference between the microphone probe tube and its pre-amplifier carriage and the horn.

Although the stepped horn differend from a theoretical exponential horn in several respects and there was an abrupt change from the 59 by 59 in. area of the horn to the smaller area of the 49 loudspeaker cones, the horn did not introduce pronounced peaks and dips in the frequency response of the system. The loading of the loudspeaker drivers was adequate to give a fairly high efficiency for the conversion of electrical power to acoustic power in the impedance tube.

All joints between the plywood sides of the horn were closely fitted and were glued and screwed together. The various segments were mounted in an enclosure filled with sand as described previously.

The electronic equipment for the driving system is listed in Table B-1, analyzing equipment is given in Table B-2.

TABLE B-1

LIST OF DRIVING EQUIPMENT

Noise Generator

Grason-Stadler Co. Model 455-B

Attenuators

Daven Attenuators

0 - 1 db in 0.1 db steps, Type 2506

0 - 10 db in 1.0 db steps, Type 2511

0 - 100 db in 10.0 db steps, Type 2513

Power Amplifier

Savage 1 kilowatt audio amplifier

Filter

General Radio--Sound and Vibration Type 1554-E Analyzer

TABLE B-2

LIST OF MEASURING EQUIPMENT

Low Frequency Impedance Tube Microphone Systems

Massa M-101 microphone

Massa M-103 preamplifier

Massa M-104 amplifier and power supply

Medium Frequency Impedance Tube Microphone Systems

Massa M-213 microphone

Massa M-114 preamplifier

Massa M-185 amplifier and power supply

Western Electro-Acoustic Lab. Type 100E amplifier

Attenuators

Daven Attenuators

0 - 1 db in 0.1 db steps, Type 2506

0 - 10 db in 1.0 db steps, Type 2511

0 - 100 db in 10.0 db steps, Type 2513

Filters

Allison variable low pass and high pass filters

Analyzer

Quan-Tech Model 303

Voltmeter

Ballantine electronic voltmeter, Model 300

Unclassified
Security Classification

DOCUMENT CONTROL DATA - R&D
(Security classification of title, body of abstract and indexing annotation must be entered when the overall report is classified)

1. ORIGINATING ACTIVITY *(Corporate author)*
IIT Research Institute
10 West 35 Street
Chicago, Illinois 60616

2a. REPORT SECURITY CLASSIFICATION
Unclassified

2b. GROUP

3. REPORT TITLE
Propagation of High Intensity Sound Waves

4. DESCRIPTIVE NOTES *(Type of report and inclusive dates)*
Final January 1966 to March 1967

5. AUTHOR(S) *(Last name, first name, initial)*
Karplus, Henry B., Raelson, Verner J., Hruska, Gale R.

6. REPORT DATE	7a. TOTAL NO. OF PAGES	7b. NO. OF REFS
September 1967	89	24

8a. CONTRACT OR GRANT NO.	9a. ORIGINATOR'S REPORT NUMBER(S)
AF 33(615)-3436 b. PROJECT NO. 4437 c. Task 443701 d.	AFFDL-TR-67-37 9b. OTHER REPORT NO(S) *(Any other numbers that may be assigned this report)*

10. AVAILABILITY/LIMITATION NOTICES
Distribution limited to U. S. Government agencies only; test and evaluation; statement applied December 1971
This document is subject to special export controls and s or foreign nationals may be made only with Division (FDD), Air Force Flight Dynamics Base, Ohio 45433.
[1] Other requests for this document must be referred to AF Flight Dynamics Laboratory, (FY), Wright-Patterson AFB, Ohio 45433

12. SPONSORING MILITARY ACTIVITY
Air Force Flight Dynamics Laboratory
Wright-Patterson AFB, Ohio 45433

13. ABSTRACT

Sound field characteristics were studied as a function of increasing intensity. It was determined that one effect outweights others. This is the distortion generated within the siren which makes it impossible to generate pure tones above a certain intensity. At high intensity the waveform of the sound assumes a sawtooth shape producing periodic shock waves. Conversely, it is concluded that if the distortion is small at the mouth of the siren, additional distortion in the subsequent propagation will not be significant. Waveforems observed in the AFFDL facility are included in an appendix.

Interaction of sound waves from different sirens will, in addition, give rise to intermodulation effects producing sum and difference frequencies. In general, the intensity in the region in which the radiation from different sirens can interact will be so much lower than the intensity in the throat of the siren horn that these effects will also be small compared with harmonic distortion generated in the sirens.

DISTRIBUTION OF THIS ABSTRACT IS UNLIMITED

DD FORM 1 JAN 64 1473

Unclassified
Security Classification

14. KEY WORDS	LINK A		LINK B		LINK C	
	ROLE	WT	ROLE	WT	ROLE	WT
Acoustic Environment						
Sound Wave Propagation						

INSTRUCTIONS

1. ORIGINATING ACTIVITY: Enter the name and address of the contractor, subcontractor, grantee, Department of Defense activity or other organization *(corporate author)* issuing the report.

2*a*. REPORT SECURITY CLASSIFICATION: Enter the overall security classification of the report. Indicate whether "Restricted Data" is included. Marking is to be in accordance with appropriate security regulations.

2*b*. GROUP: Automatic downgrading is specified in DoD Directive 5200.10 and Armed Forces Industrial Manual. Enter the group number. Also, when applicable, show that optional markings have been used for Group 3 and Group 4 as authorized.

3. REPORT TITLE: Enter the complete report title in all capital letters. Titles in all cases should be unclassified. If a meaningful title cannot be selected without classification, show title classification in all capitals in parenthesis immediately following the title.

4. DESCRIPTIVE NOTES: If appropriate, enter the type of report, e.g., interim, progress, summary, annual, or final. Give the inclusive dates when a specific reporting period is covered.

5. AUTHOR(S): Enter the name(s) of author(s) as shown on or in the report. Enter last name, first name, middle initial. If military, show rank and branch of service. The name of the principal author is an absolute minimum requirement.

6. REPORT DATE: Enter the date of the report as day, month, year; or month, year. If more than one date appears on the report, use date of publication.

7*a*. TOTAL NUMBER OF PAGES: The total page count should follow normal pagination procedures, i.e., enter the number of pages containing information.

7*b*. NUMBER OF REFERENCES: Enter the total number of references cited in the report.

8*a*. CONTRACT OR GRANT NUMBER: If appropriate, enter the applicable number of the contract or grant under which the report was written.

8*b*, 8*c*, & 8*d*. PROJECT NUMBER: Enter the appropriate military department identification, such as project number, subproject number, system numbers, task number, etc.

9*a*. ORIGINATOR'S REPORT NUMBER(S): Enter the official report number by which the document will be identified and controlled by the originating activity. This number must be unique to this report.

9*b*. OTHER REPORT NUMBER(S): If the report has been assigned any other report numbers *(either by the originator or by the sponsor)*, also enter this number(s).

10. AVAILABILITY/LIMITATION NOTICES: Enter any limitations on further dissemination of the report, other than those imposed by security classification, using standard statements such as:

(1) "Qualified requesters may obtain copies of this report from DDC."

(2) "Foreign announcement and dissemination of this report by DDC is not authorized."

(3) "U. S. Government agencies may obtain copies of this report directly from DDC. Other qualified DDC users shall request through

_____."

(4) "U. S. military agencies may obtain copies of this report directly from DDC. Other qualified users shall request through

_____."

(5) "All distribution of this report is controlled. Qualified DDC users shall request through

_____."

If the report has been furnished to the Office of Technical Services, Department of Commerce, for sale to the public, indicate this fact and enter the price, if known.

11. SUPPLEMENTARY NOTES: Use for additional explanatory notes.

12. SPONSORING MILITARY ACTIVITY: Enter the name of the departmental project office or laboratory sponsoring *(paying for)* the research and development. Include address.

13. ABSTRACT: Enter an abstract giving a brief and factual summary of the document indicative of the report, even though it may also appear elsewhere in the body of the technical report. If additional space is required, a continuation sheet shall be attached.

It is highly desirable that the abstract of classified reports be unclassified. Each paragraph of the abstract shall end with an indication of the military security classification of the information in the paragraph, represented as *(TS), (S), (C), or (U)*.

There is no limitation on the length of the abstract. However, the suggested length is from 150 to 225 words.

14. KEY WORDS: Key words are technically meaningful terms or short phrases that characterize a report and may be used as index entries for cataloging the report. Key words must be selected so that no security classification is required. Identifiers, such as equipment model designation, trade name, military project code name, geographic location, may be used as key words but will be followed by an indication of technical context. The assignment of links, rules, and weights is optional.